Workshop, June 15–19, Physics Division
at Argonne National Laboratory

Argonne NATIONAL LABORATORY

QCD BOUND STATES: METHODS & PROPERTIES

Connecting Dalitz plots and hadronic models in heavy-meson decays

Bruno El-Bennich

Physics Division @ Argonne National Laboratory

Season Home Game

Sakharov's (necessary) conditions to create baryon-antibaryon asymmetry in the universe

- Baryon number *B* violation
- *C*-symmetry and *CP*-symmetry violation.
- Interactions out of thermal equilibrium.

A. D. Sakharov, "*Violation of CP invariance, C asymmetry, and baryon asymmetry of the universe*", *Soviet Physics Journal of Experimental and Theoretical Physics (JETP)* **5**: 24–27 (1967).

What is needed in order to generate *CP* violation?

- Decay amplitudes must contain weak as well as strong phases:

$$\mathcal{A}(A \to B) = g_1 r_1 e^{i\phi_1} + g_2 r_2 e^{i\phi_2}$$
$$\bar{\mathcal{A}}(\bar{A} \to \bar{B}) = g_1^* r_1 e^{i\phi_1} + g_2^* r_2 e^{i\phi_2}$$

- The *CP* violating difference in these two processes is:

$$|\mathcal{A}|^2 - |\bar{\mathcal{A}}|^2 = 2\, r_1 r_2 \,\mathrm{Im}\, g_1 g_2^* \sin(\phi_1 - \phi_2)$$

and *CP* violation occurs only if $\left|\frac{\bar{\mathcal{A}}}{\mathcal{A}}\right| \neq 1$

Motivation

- First observation of *direct CP* violation in *non-leptonic three-body B decays* of +30±11% (Belle,3.9σ) and +44±10±4% (BaBar, 3.7σ) in the decay $B \to \rho K,\ \rho \to \pi\pi$.
- Three-body *B* and *D* decays allow for a detailed study of scalar resonances in pion-pion and pion-kaon pairs in *S*-waves.
- The decays of *heavy* mesons into two or three light mesons provide us with a theoretical laboratory to study in detail electroweak physics but ***also*** non-perturbative hadronic physics.
- Despite important theoretical progress in perturbative QCD, uncertainties of hadronic nature still blur these successes: *how well are the strong phases known in these decays?*
- This lack of accurate knowledge is (still) an obstacle to the precision determination of the CKM angles α and γ as well as any signals from physics beyond the Standard Model.

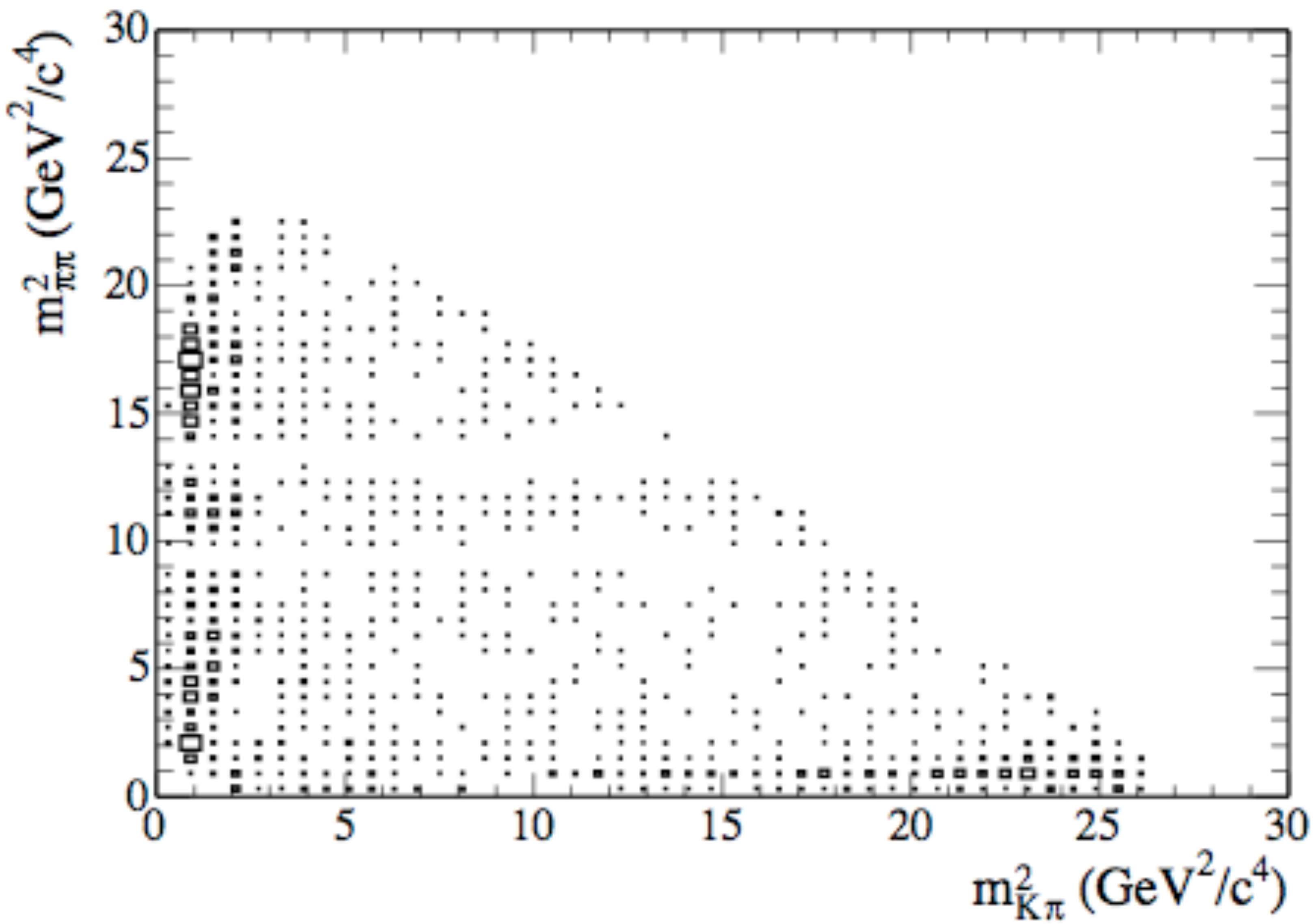

FIG. 2: Background subtracted Dalitz plot of the combined $B^{\pm} \to K^{\pm}\pi^{\mp}\pi^{\pm}$ data sample in the signal region. The plot shows bins with greater than zero entries, the area of the boxes being proportional to the number of entries.

Evidence for scalar (and other) resonances in hadronic charmless $B \to K\pi\pi$ decays

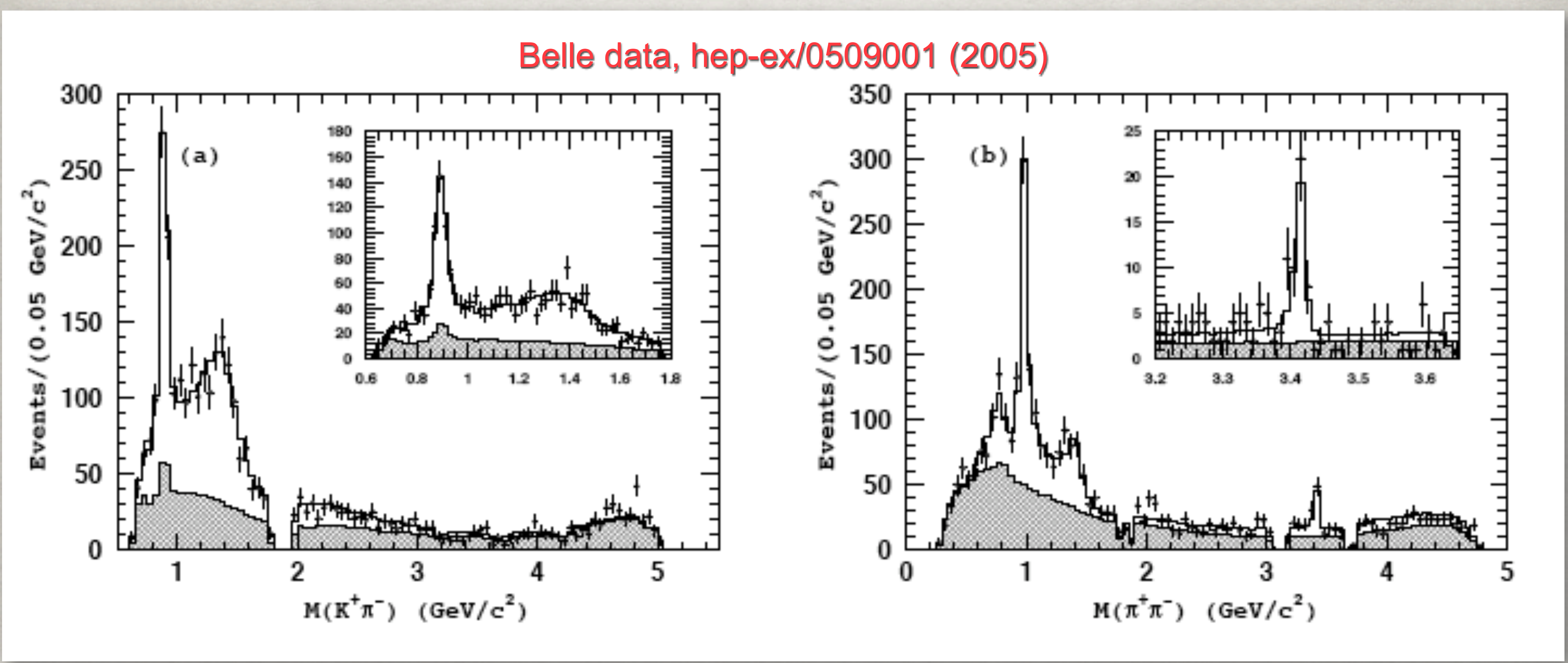

BaBar Collaboration, arXiv:0803.4451

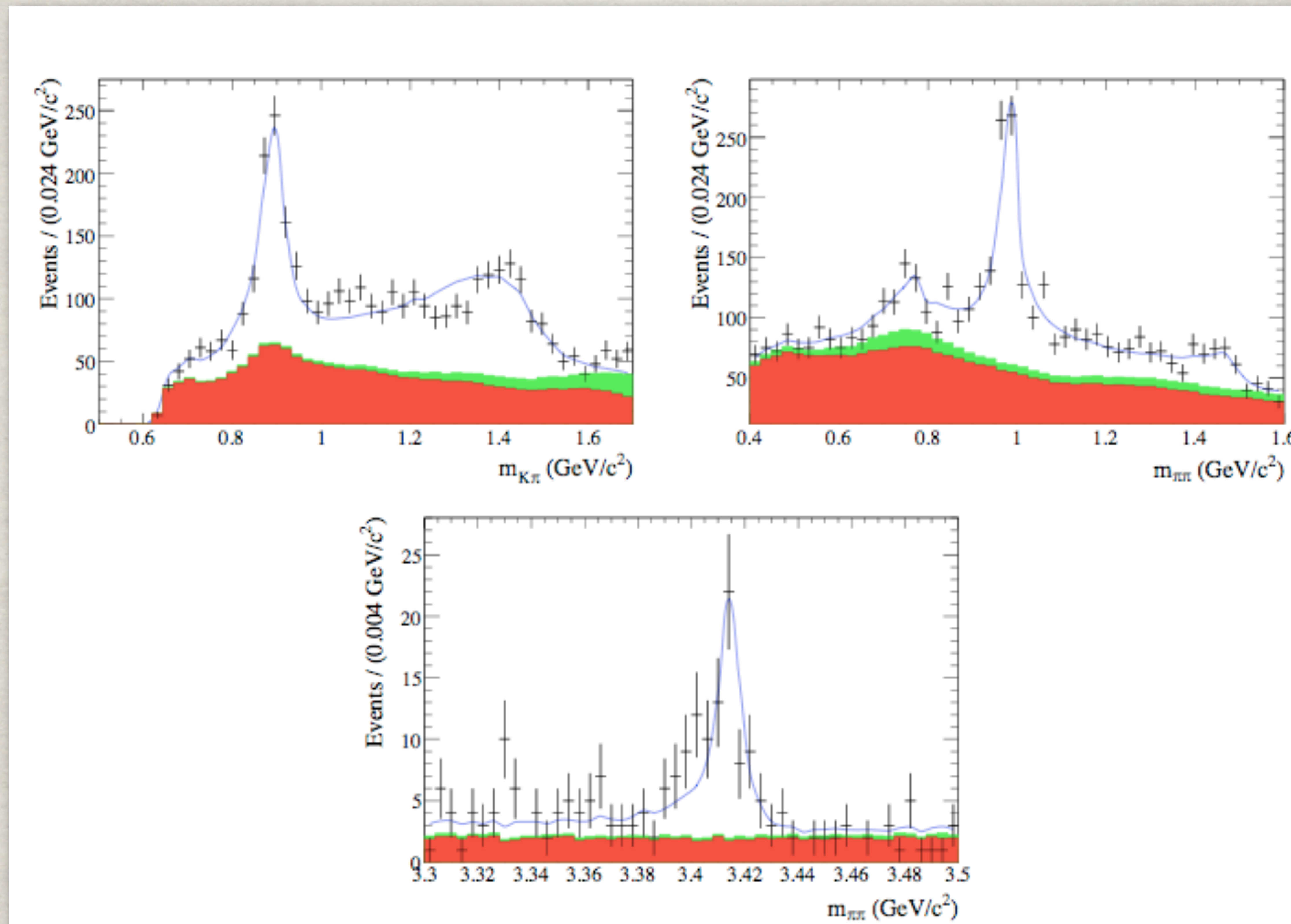

$D \to \pi\pi\pi$ decays

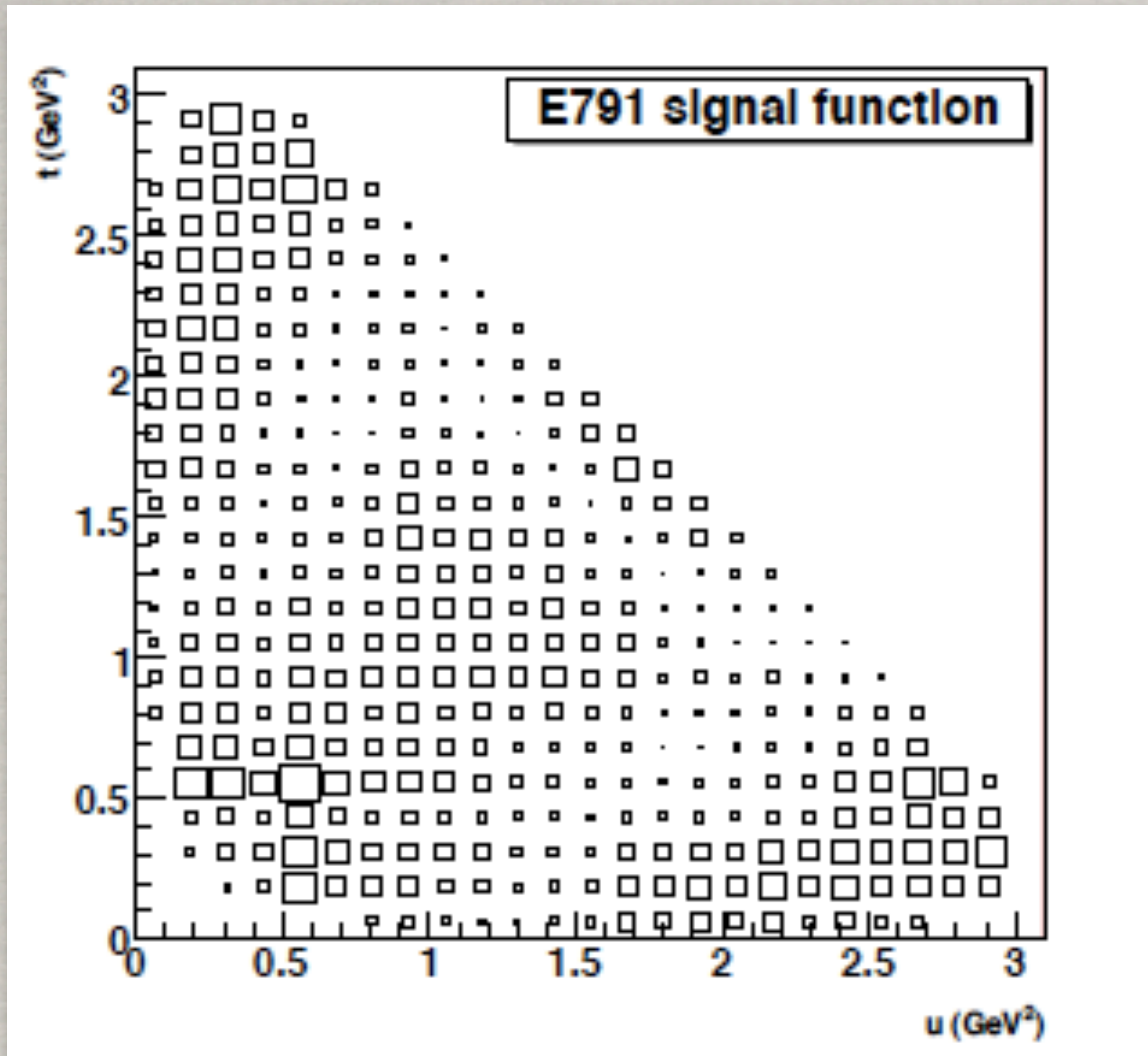

Summary of the results (errors are omitted)

Resonance	Fit Fraction (%)	Mag.	Phase (°)
$\sigma(500)$	46.3	1.17	205.7
$\rho^0(770)$	33.6	1	0
NR	7.8	0.48	57.3
$f_0(980)$	6.2	0.43	165.0
$f_2(1270)$	19.4	0.76	165.0
$f_0(1370)$	2.3	0.26	105.4
$\rho^0(1400)$	0.7	0.14	319.1

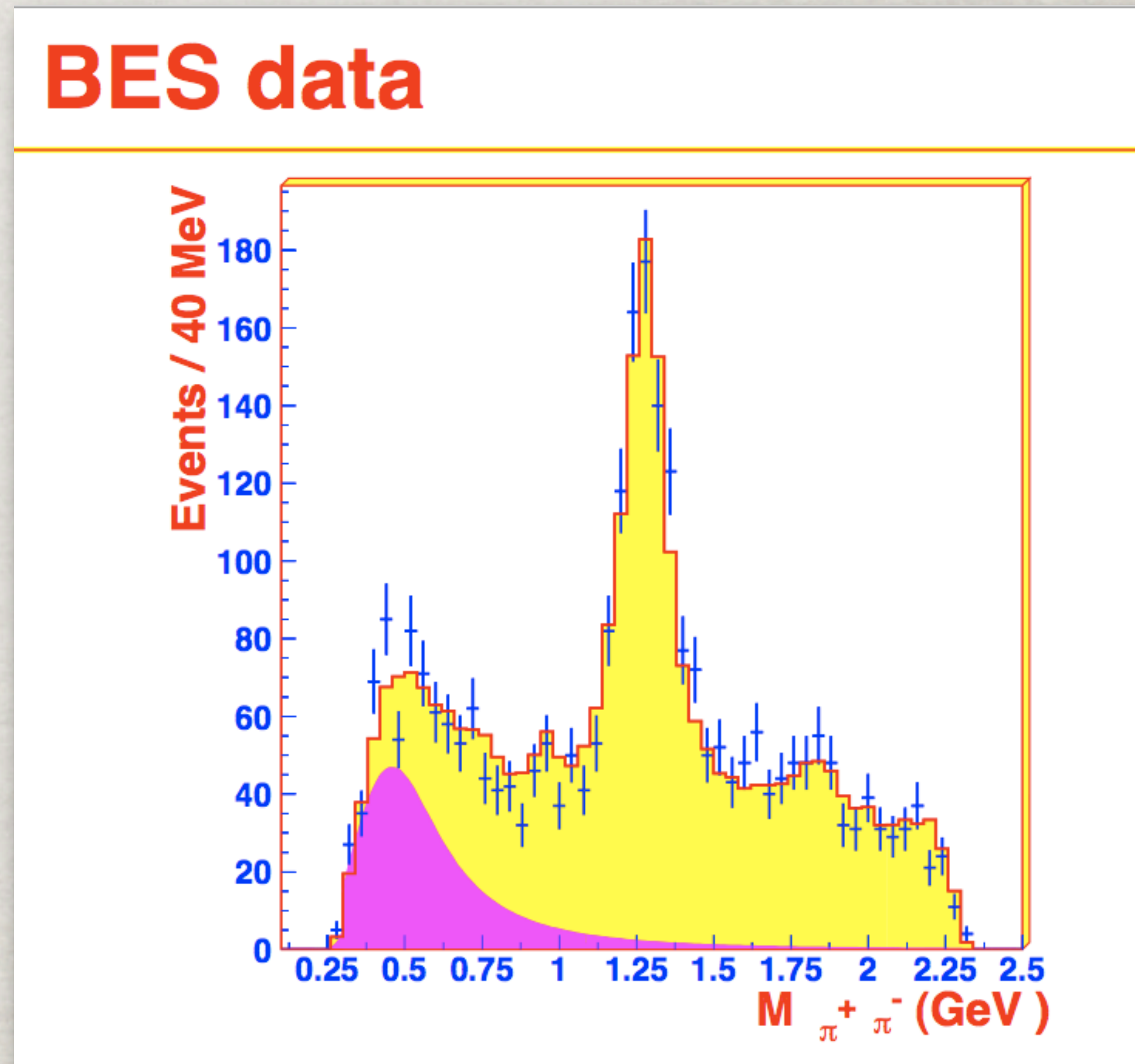

A typical example for the isobar model parametrization of the $B^{\pm}\to K^{\pm}\pi^{+}\pi^{-}$ Dalitz plot

The decay amplitude is parametrized by a coherent sum (Belle parametrization):

$$
\begin{aligned}
&\mathcal{M}(B^{\pm}\to K^{\pm}\pi^{\pm}\pi^{\mp}) = \\
&\quad = a_{K^*}e^{i\delta_{K^*}}(1\pm b_{K^*}e^{i\varphi_{K^*}})\mathcal{A}(K^*(892)^0) + a_{K_0^*}e^{i\delta_{K_0^*}}(1\pm b_{K_0^*}e^{i\varphi_{K_0^*}})\mathcal{A}(K_0^*(1430)^0) \\
&\quad + \ a_\rho e^{i\delta_\rho}(1\pm b_\rho e^{i\varphi_\rho})\mathcal{A}(\rho(770)^0) + a_\omega e^{i\delta_\omega}(1\pm b_\omega e^{i\varphi_\omega})\mathcal{A}(\omega(782)) \\
&\quad + \ a_{f_0}e^{i\delta_{f_0}}(1\pm b_{f_0}e^{i\varphi_{f_0}})\mathcal{A}_{\mathrm{Flatte}}(f_0(980)) + a_{f_2}e^{i\delta_{f_2}}(1\pm b_{f_2}e^{i\varphi_{f_2}})\mathcal{A}(f_2(1270)) \\
&\quad + \ a_{f_X}e^{i\delta_{f_X}}(1\pm b_{f_X}e^{i\varphi_{f_X}})\mathcal{A}(f_X) + a_{\chi_{c0}}e^{i\delta_{\chi_{c0}}}(1\pm b_{\chi_{c0}}e^{i\varphi_{\chi_{c0}}})\mathcal{A}(\chi_{c0}) \\
&\quad + \ \mathcal{A}_{\mathrm{nr}}(K^{\pm}\pi^{\pm}\pi^{\mp})
\end{aligned}
$$

where the amplitudes a_i and b_i, relative phase parameters ϕ_i, δ_i for $i = f_0(980)$, $\rho^0(770), \omega(782), K^*(892), K_0^*(1430), f_2(1270), f_X(1300)\ldots$ as well as mass parameters are fitted to the Dalitz plot for $K^{\pm}\pi^{\pm},\pi^{\mp}$ events in the signal region.

$\mathcal{A}_{nr}$ describes the non-resonant $\pi^{\pm}\pi^{\mp}$ and $K^{\pm}\pi^{\mp}$ amplitudes; the other amplitudes $\mathcal{A}_i$ are line shapes taken to be Breit-Wigner functions (except for the $f_0(980)$ where a Flatté function is used).

Weak decay amplitudes

What is the quasi two-body approach?

Examples of *quasi two-body* reactions:

$B^{\pm} \rightarrow f_0(980)K^{\pm}$ followed by the hadronic decays $f_0(980) \rightarrow (\pi^+\pi^-)_S$ or $f_0(980) \rightarrow (K^+K^-)_S$ with the meson pairs in an *S-wave, I=0* state.

$B^{\pm} \rightarrow K_0^*(1430)\pi^{\pm}$ followed by the hadronic decay $K_0^*(1430) \rightarrow (K^{\pm}\pi^{\mp})_S$ in an *S-wave, I=1/2* state.

The Beauty meson - a cartoon

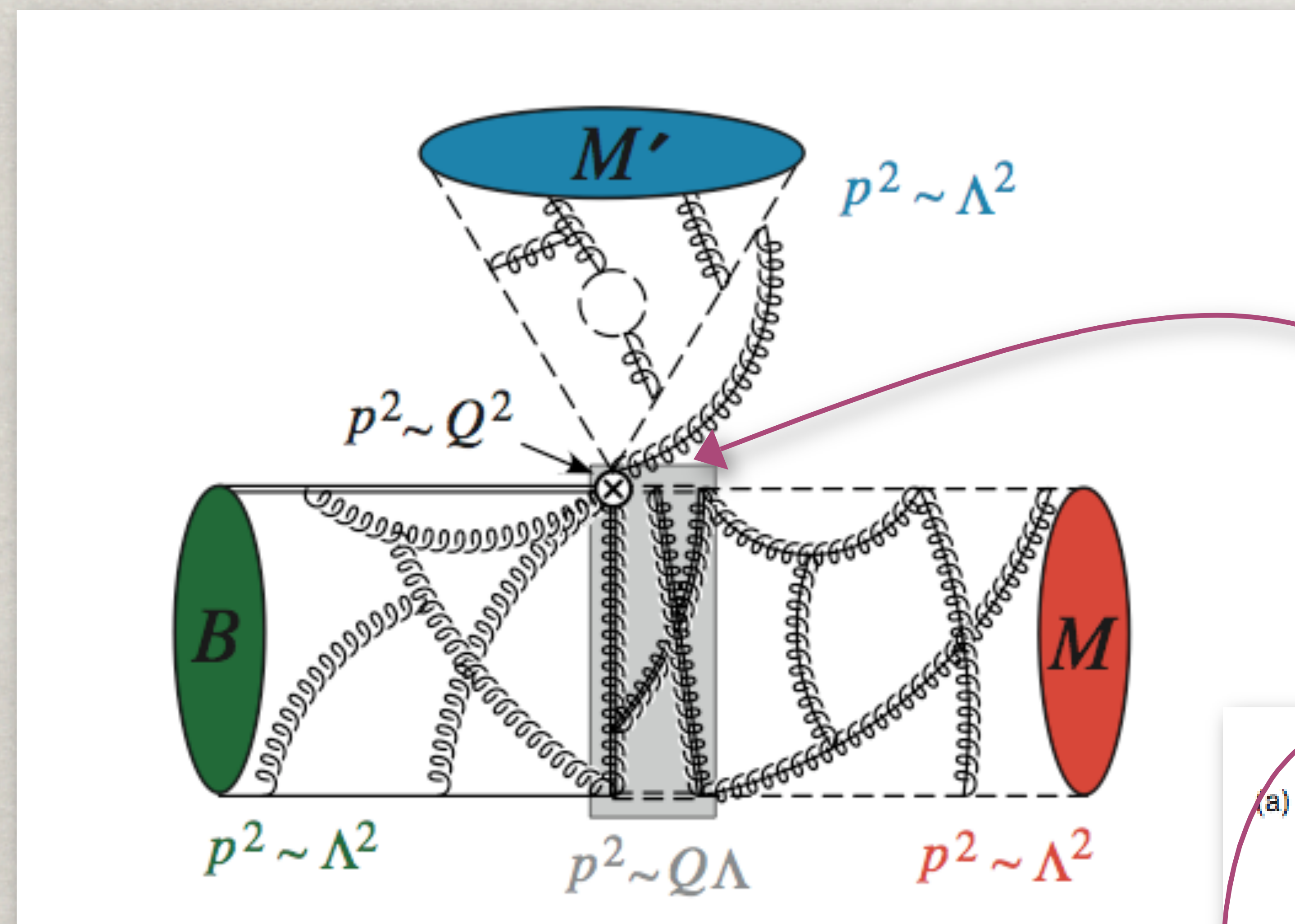

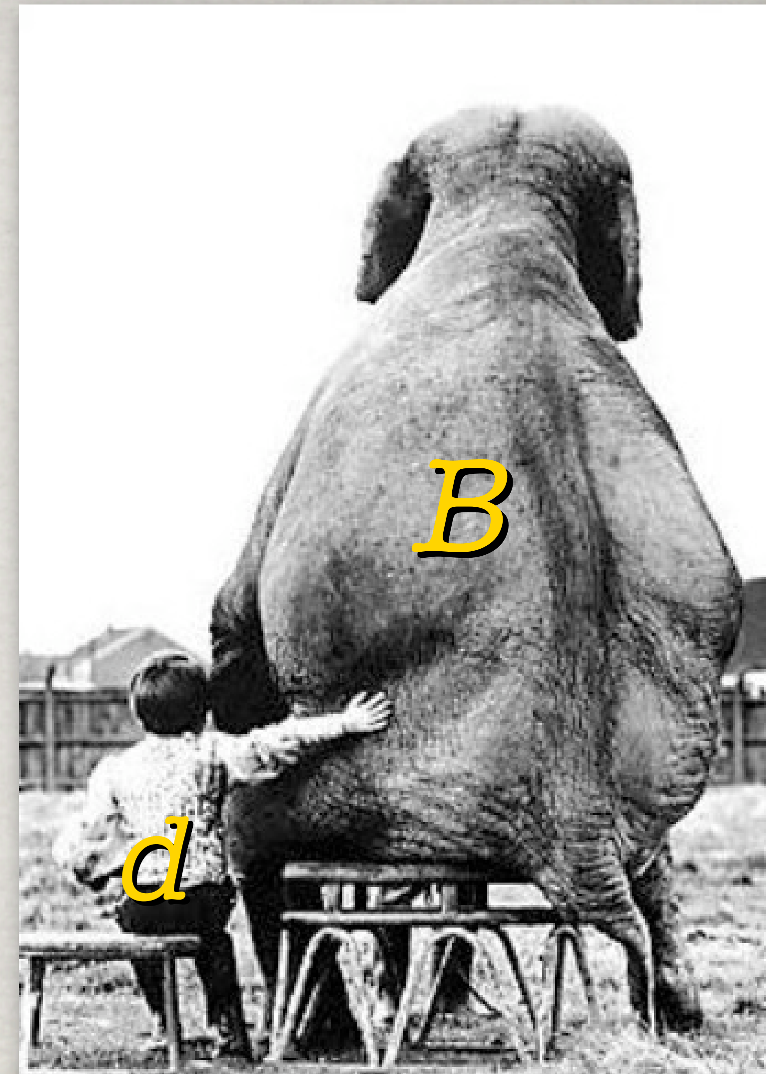

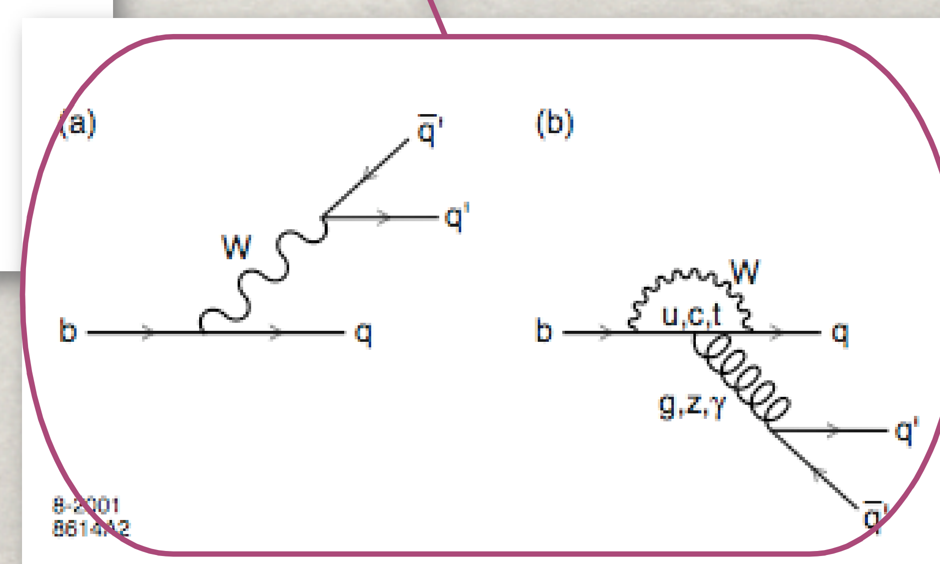

Weak effective Hamiltonian

Sum of local operators Q_i multiplied by short-range Wilson coefficients $C_i(\mu)$ and CKM matrix elements:

$$\mathcal{H} = \frac{G_F}{\sqrt{2}}\left[V_{ub}V_{us}^*(C_1(\mu)O_1^u + C_2(\mu)O_2^u) - V_{tb}V_{ts}^*\sum_{i=3}^{10} C_i(\mu)O_i\right]$$

O_1 and O_2 are left-handed current-current operators, for example:

$$O_1^u = \bar{s}_\alpha\gamma_\mu(1-\gamma_5)u_\alpha\bar{u}_\beta\gamma_\mu(1-\gamma_5)b_\beta$$

O_3 …. O_{10} are QCD and electroweak penguin operators, for instance:

$$O_4 = \bar{s}_\alpha\gamma_\mu(1-\gamma_5)b_\beta\sum_{q=u,d,s,c}\bar{q}_\beta\gamma_\mu(1-\gamma_5)q_\alpha$$

QCD factorization

$$\langle M_1^* M_2 | H_{\text{eff}} | B \rangle = \frac{G_F}{\sqrt{2}} V_{\text{CKM}} \sum_k C_k(\mu) \langle M_1^* M_2 | O_k(\mu) | B \rangle$$

G_F = 1.166 x 10^{-5} GeV^{-2} = Fermi constant
V_{CKM} = CKM matrix element, μ = renormalisation scale

- $C_k(\mu)$ perturbative Wilson coeffi cients: short range physics, scale dependent "couplings" associated to the vertices $O_k(\mu)$.
- $\langle M_1 M_2 | O_k(\mu) | B \rangle$ non-perturbative hadronic matrix elements: long distance physics.
- $O_k(\mu)$ local operators - electroweak interaction + QCD - govern "effectively" the decay - main task theory: compute these hadronic matrix elements in a reliable way.

Factorization schematically

Beneke, Buchalla, Neubert, Sachrajda, Phys. Rev. Lett. 83, 1914 (1999); Nucl. Phys. B 591, 313 (2000); Nucl. Phys. B 606, 245 (2001); *Beneke & Neubert*, Nucl. Phys. B 675, 333 (2003).

$$\langle (M_1 M_2)_{S,P} M_3 | Q_k(\mu) | B \rangle \sim \langle (M_1 M_2)_{S,P} | J_1 | 0 \rangle \otimes \langle M_3 | J_2 | B \rangle \times \left[1 + \sum_n r_n \alpha_s^n + \mathcal{O}(\Lambda_{\mathbf{QCD}}/m_b) \right]$$

Radiative vertex corrections and hard gluon exchange with spectator quark

Scalar or vector form factor; their definition allows for inclusion of pion-pion and kaon-pion form factors and the calculation of 'resonance decay constant'

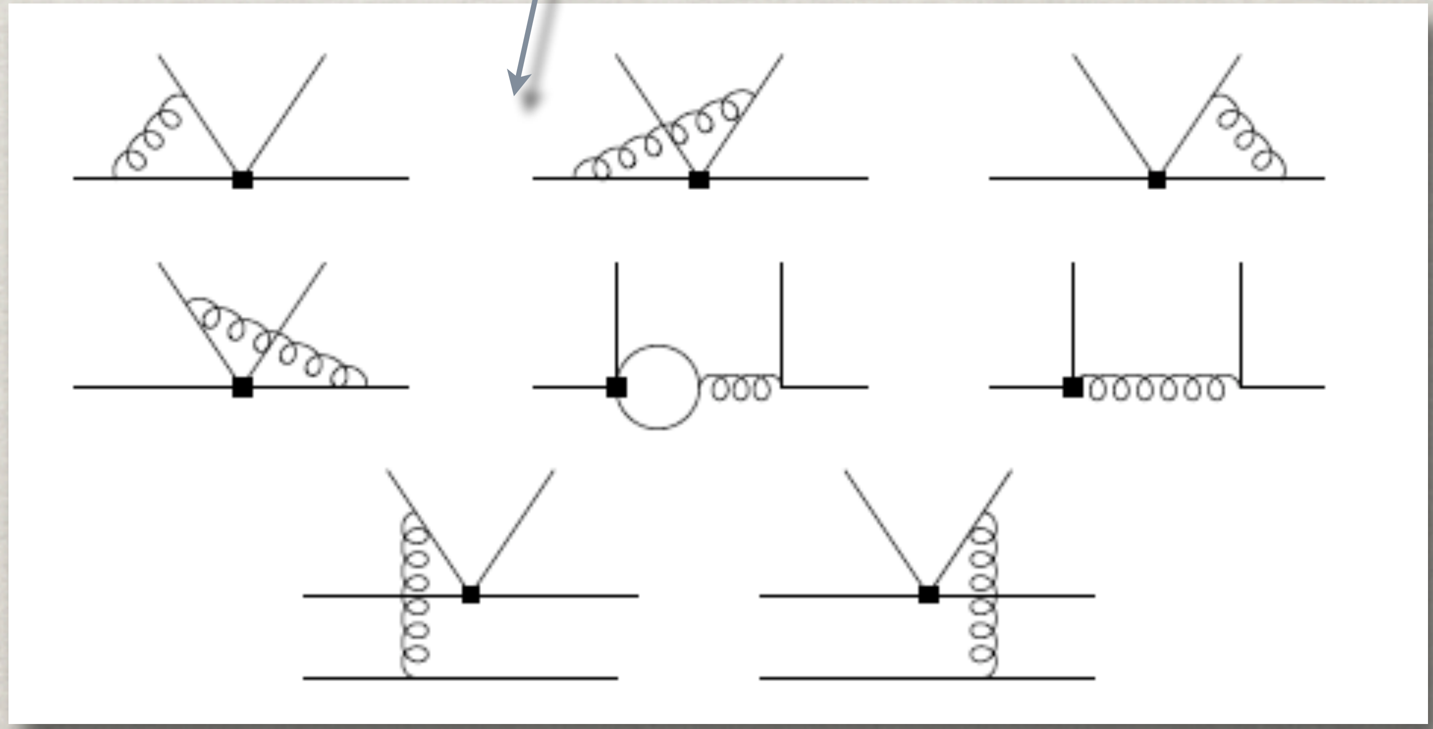

- In the two-body approach QCD factorization predictions for branching ratios compare rather well with experiment for two final pseudoscalar meson states *without* strangeness.

- Already in the penguin dominated decays $B \to K\pi$ the theoretical amplitudes give too low branching ratios if some phenomenological parameters, introduced due to endpoint divergences in annihilation and spectator hard-scattering amplitudes, are not fine tuned.

- For quasi two-body final states, such as $\varrho(770)K$, $f_0(980)K$, $K_0^*(1430)\pi$, $K^*(892)\pi$, this approach compares poorly with experimental BRs unless phenomenological amplitudes are introduced in the weak decay amplitudes.

- By poor is meant a factor 2 to 5 in the BRs, see for instance Beneke & Neubert, Nucl. Phys. B675, 333 (2003); Cheng *et al.*, Phys. Rev. D 76, 094006 (2007). El-Bennich *et al.*, Phys. Rev. D 79, 094005 (2009).

- We propose improvements in precision of heavy-to-light transition form factors as well as scalar and vector form factors which take into account pion-pion and pion-kaon rescattering that follow the resonance.

Hadronic form factors

The case of scalar and vector kaons in the final state

Calculated in QCD-factorization

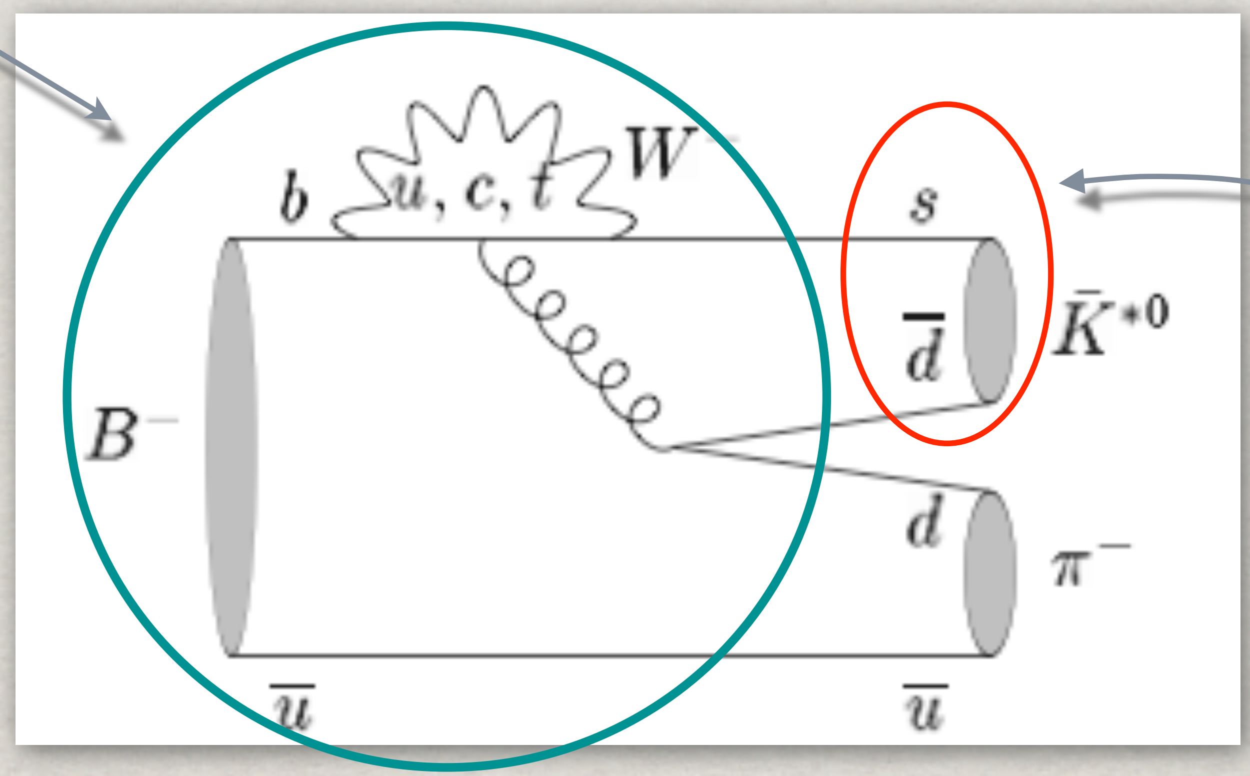

Scalar or vector form factor

➟ *no tree digrams, only QCD and electroweak penguins*

B. El-Bennich, A. Furman, R. Kaminski, L. Lesniak, B. Loiseau and B. Moussallam, Phys. Rev. D79, 094005 (2009).

Scalar and vector meson-meson form factors which describe FSI

Introduce scalar and vector form factors $f_0(q^2)$ and $f_1(q^2)$:

in S- and *P*-wave

$$\langle K^-(p_{K^-})\pi^+(p_{\pi^+})|\bar{s}\gamma_\mu(1-\gamma_5)d|0\rangle =$$

$$= \left[(p_{K^-}-p_{\pi^+})_\mu - \frac{m_K^2-m_\pi^2}{q^2}q_\mu\right] f_1^{K^-\pi^+}(q^2) + \frac{m_K^2-m_\pi^2}{q^2}q_\mu f_0^{K^-\pi^+}(q^2)$$

- ✦ The interaction of the ππ or π*K* pair which form the resonance with the third meson is power suppressed in $\Lambda_{\rm QCD}/m_b$ and neglected here.
- ✦ A coupled-channel (unitary!) *T*-matrix which includes main resonances observed in the pion-pion and pion-kaon invariant mass distributions based on coupled Omnès-Mushkelishvili integral equations.
- ✦ *T*-matrix is parametrized with experimental data on pion and kaon production (LASS); constraints from chiral perturbation theory imposed at low energy and from asymptotic QCD (Brodsky-Lepage).

Definition of scalar and vector πK form factors

$$\langle K^+(p_K)|\bar{u}\gamma^\mu s|\pi^0(p_\pi)\rangle = f_+^{K^+\pi^0}(t)\,(p_K+p_\pi)^\mu + f_-^{K^+\pi^0}(t)\,(p_K-p_\pi)^\mu$$

with $t = (p_K - p_\pi)^2$

which is related to the scalar form factor (πK in S-wave),

$$f_0 \equiv F_1(t) = \sqrt{2}\left[f_+^{K^+\pi^0}(t) + \frac{t}{m_K^2 - m_\pi^2} f_-^{K^+\pi^0}(t)\right]$$

and vector form factor (πK in P-wave):

$$f_1(t) \equiv G_1(t) \equiv f_+(t) = \sqrt{2} f_+^{K^+\pi^0}(t)$$

These form factors also appear in semileptonic decays $\tau \to K\pi\nu_\tau$ or $K \to \pi l \nu_l$

B. Moussallam, **Eur.Phys.J.C53:401-412 (2008).**

M. Jamin, J. Oller & A. Pich, **Nucl.Phys.B622:279-308 (2002).**

What do we know about πK scattering?

We can make use knowledge from pion and kaon production experiments (LASS data)

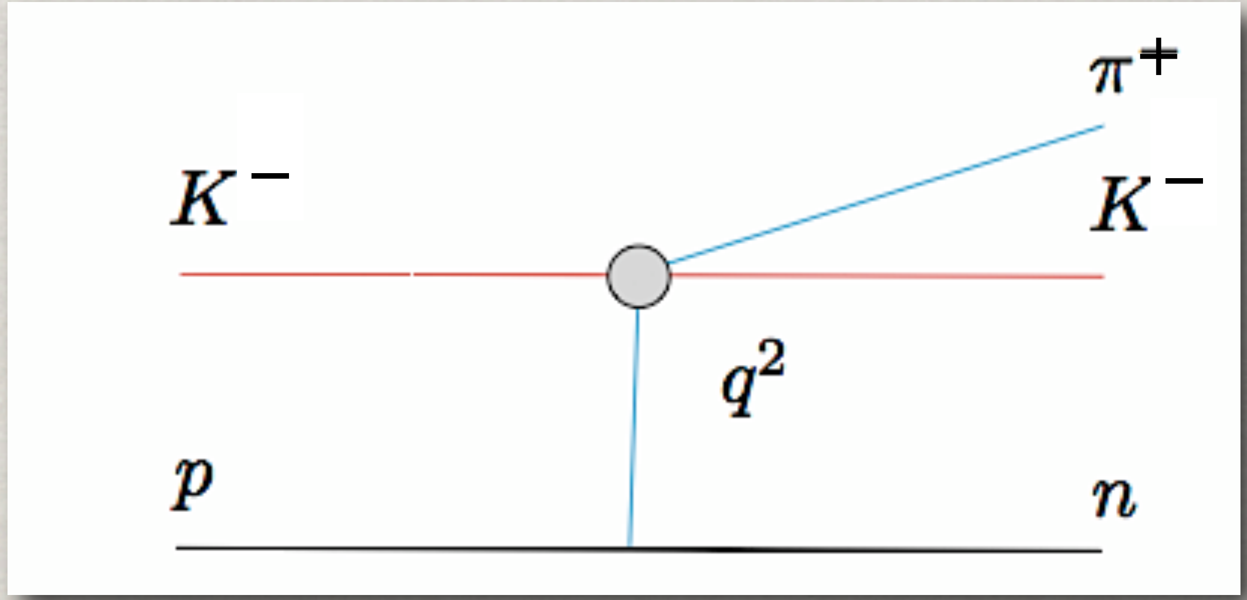

High statistics experiments: Estabrooks (1979), Hyams (LASS 1988)
In the case of $\pi K \rightarrow \pi K$: δ_l and η_l determined for $l = 0,1 \ldots 5$
Energy domain: 0.8 GeV < E < 2.5 GeV

More recent data on $D \rightarrow \pi K \nu l$: $\delta_0 - \delta_1$ determined (FOCUS collab.)

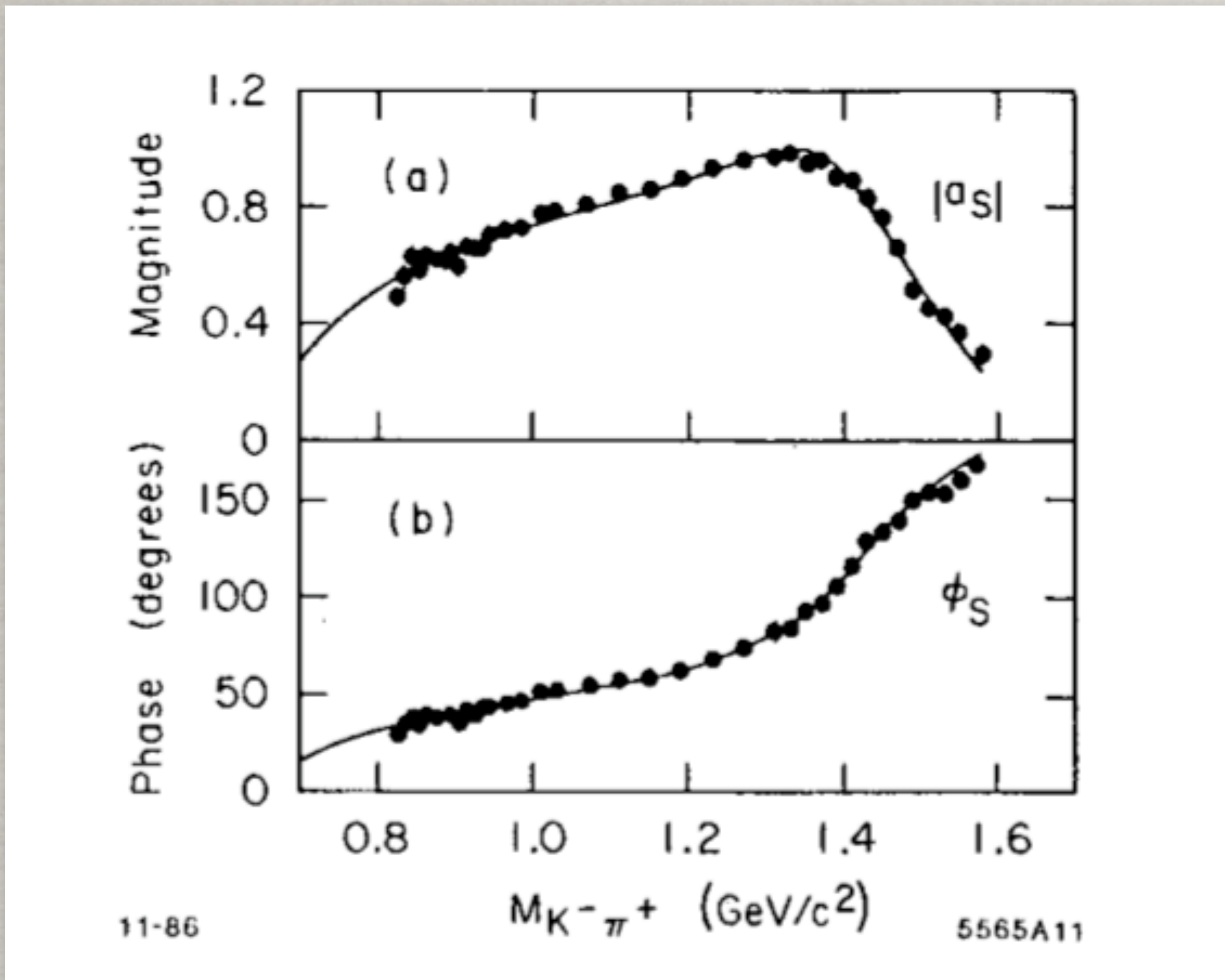
1.2
0.8
0.4
0
Magnitude
(a)
$|a_S|$
150
100
50
0
Phase (degrees)
(b)
ϕ_S
0.8
1.0
1.2
1.4
1.6
$M_{K^-\pi^+}$ (GeV/c^2)
11-86
5565A11

P-wave

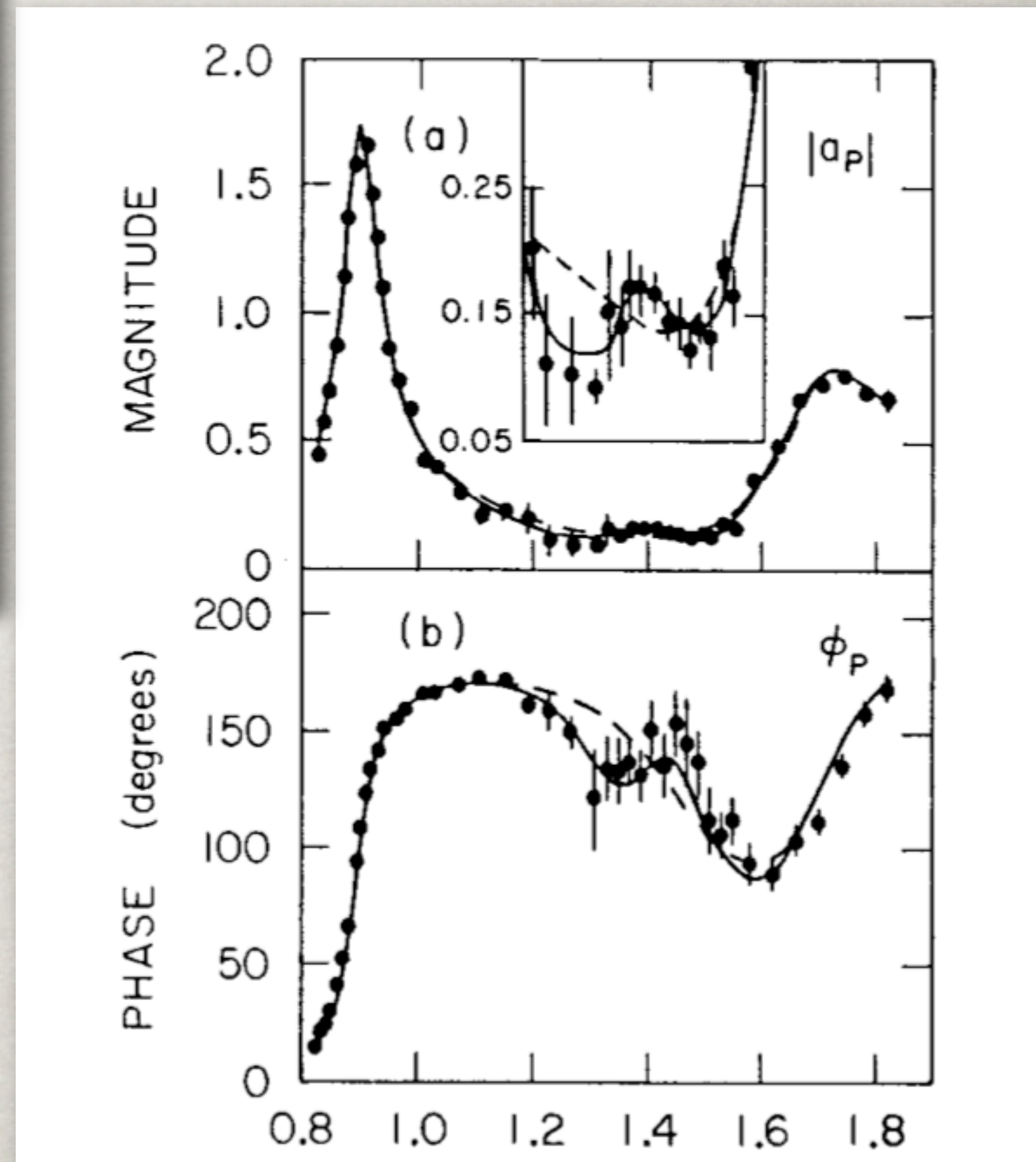
2.0
1.5
1.0
0.5
0
MAGNITUDE
(a)
$|a_P|$
0.25
0.15
0.05
200
150
100
50
0
PHASE (degrees)
(b)
ϕ_P
0.8
1.0
1.2
1.4
1.6
1.8

S-wave

Dominant inelastic channels for $E \lesssim 2.5$ GeV: **LASS (1987), LASS (1984)**

$-\, l = 0$	$K\eta'$ dominant	
$-\, l = 1$	$K^*\pi$	via $K^*(1410)$
	$K^*\pi$, $K\rho$	via $K^*(1680)$

Remark: little $l = 1$ coupling via resonances in $K\eta$ and $K\eta'$.

This introduces two more matrix elements:

$$\langle K^{*+}(p_V,\lambda)|\bar{u}\gamma_\mu s|\pi^0(p_\pi)\rangle = \epsilon_{\mu\nu\alpha\beta}\, e^{*\nu}(\lambda) p_V^\alpha p_\pi^\beta \; H_2(t)$$

$$\langle \rho^0(p_V,\lambda)|\bar{u}\gamma_\mu s|K^-(p_K)\rangle = -\epsilon_{\mu\nu\alpha\beta}\, e^{*\nu}(\lambda) p_V^\alpha p_K^\beta \; H_3(t)$$

Mushkelishvili-Omnès Equations

Analyticity and asymptotic conditions: ***dispersion relation without subtraction***

$$\mathrm{Re}\ F_1(t) = \frac{1}{\pi}\int_{(m_\pi+m_K)^2}^{\infty} \frac{\mathrm{Im}\ F_1(t')}{t'-t}\,dt' \qquad \text{(scalar form factor)}$$

$$\mathrm{Re}\ G_1(t) = \frac{1}{\pi}\int_{(m_\pi+m_K)^2}^{\infty} \frac{\mathrm{Im}\ G_1(t')}{t'-t}\,dt' \qquad \text{(vector form factor)}$$

Unitarity equations and *T*-invariance:

$$\mathrm{Im}\, F_m(t) = \frac{1}{2}\sum_n T^*_{mn}(t) F_n(t) \qquad \mathrm{Im}\, G_m(t) = \frac{1}{2}\sum_n T^*_{mn} G_n(t)$$

with the approximation of the truncation $|n\rangle = |K\pi\rangle, |K\eta'\rangle$ for the scalar $F_1(t)$ and $|n\rangle = |K\pi\rangle, |K^*\pi\rangle, |K\rho\rangle$ for the vector $G_1(t)$.

Combining the dispersion relations with the unitarity equations yields a set of integral equations (Mushkelishvili-Omnès) which can be solved numerically with *initial conditions*.

➟ Find an effective parametrization of T_{mn}(t) constrained by theory (chiral symmetry) at low energies and experimental data on phase shifts and inelasticities at higher energies.

Theoretical contraints on form factors

* $t = 0$ **Chiral symmetry constraints**

$G_1(0)$: $= 1 + O((m_s - m)^2)$ Ademollo-Gatto (1964)

$= 0.987 + O((m_s - m)^3)$ Gasser-Leutwyler(1985)

$H_2,\ H_3$: $H_2(0) = (1.54 \pm 0.08)\ GeV^{-1}$ Chiral limit $(\rho^+ \to \gamma\pi^+)$

$H_3(0) = (-1.54 \pm 0.08\ GeV^{-1}$

$H_2(0) = (1.41 \pm 0.09 - 65.4\,a)\ GeV^{-1}$ with $O(m_s, \hat{m})$ correc.

$H_3(0) = (-1.34 \pm 0.07 - 65.4\,a)\ GeV^{-1}$ a= $O(10^{-3})$

* $t = \infty$ QCD, Brodsky-Lepage (1980)

$$G_1(-Q^2)\Big|_{Q^2\to\infty} \sim \frac{16\pi\sqrt{2}\,\alpha_s(Q^2)F_\pi^2}{Q^2}$$

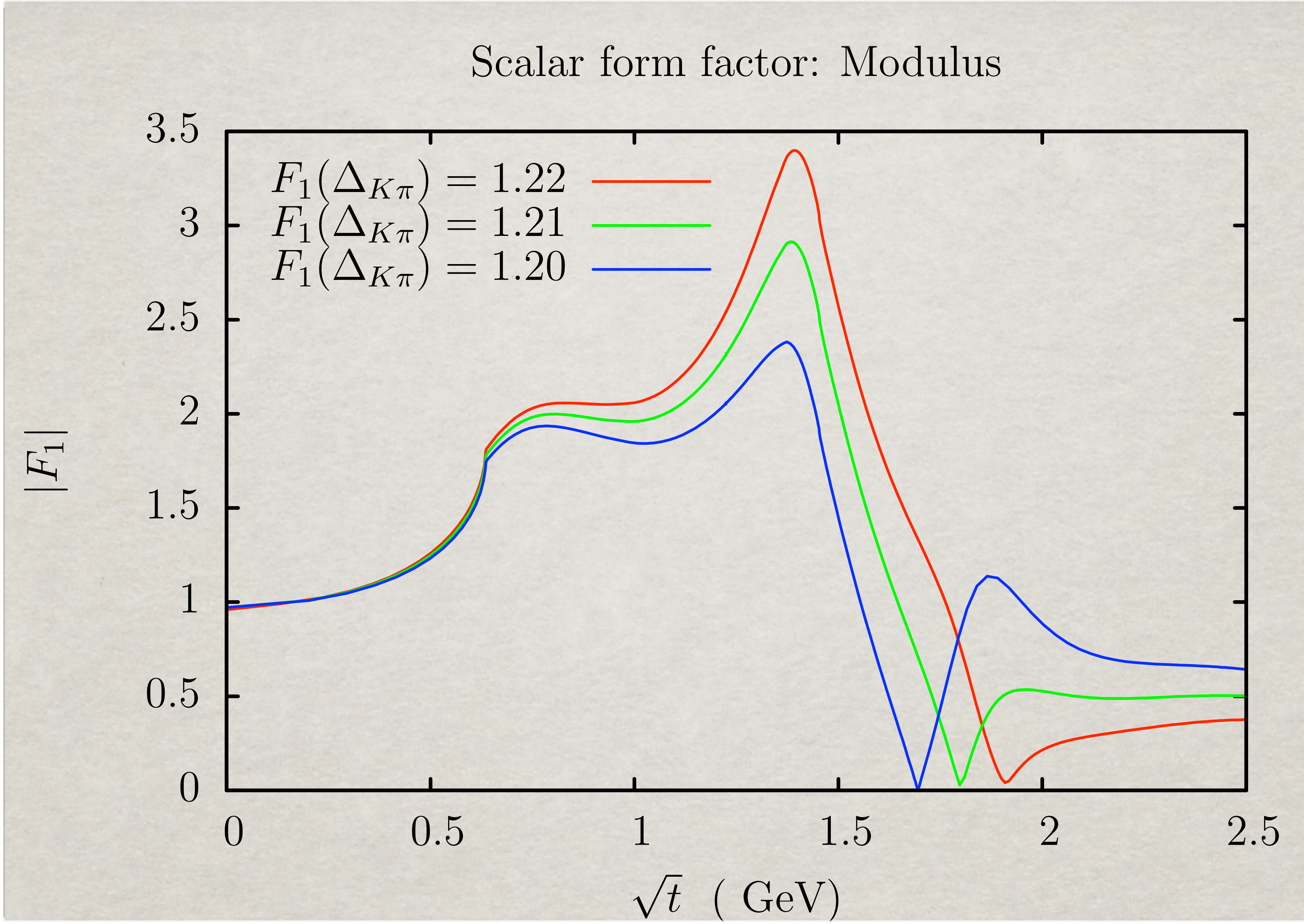

Solving the Muskhelishvili-Omnès equations for $F_1(t)$ requires two initial conditions near $t = 0$. One is the Cheng-Dashen point at $t = \Delta_{K\pi} = m_K^2 - m_\pi^2$.

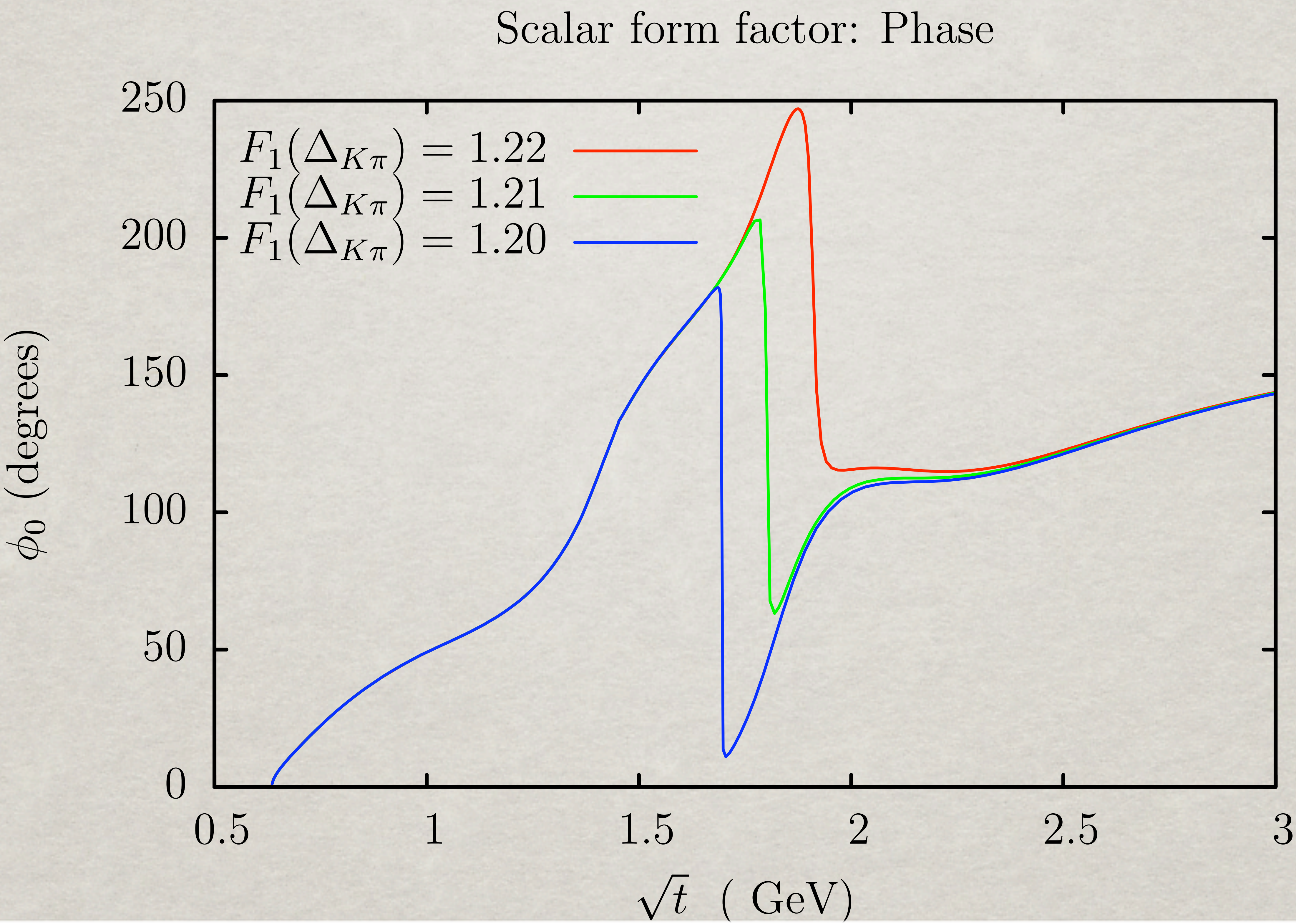

Scalar form factor: Phase
$F_1(\Delta_{K\pi}) = 1.22$
$F_1(\Delta_{K\pi}) = 1.21$
$F_1(\Delta_{K\pi}) = 1.20$
ϕ_0 (degrees)
$\sqrt{t}$ (GeV)
0
50
100
150
200
250
0.5
1
1.5
2
2.5
3

Vector form factor $\longrightarrow \pi K$ in P -wave

$$G_1(t) \equiv f_+(t) = \sqrt{2} f_+^{K^+\pi^0}(t)$$

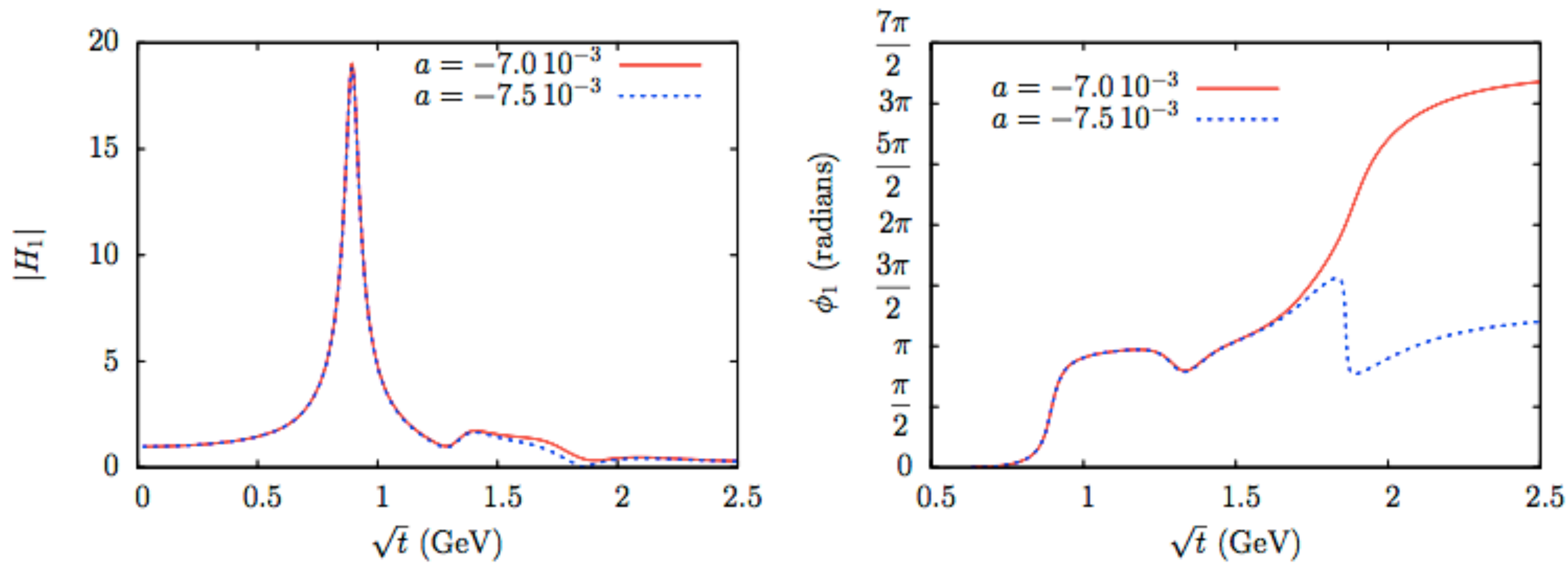

FIG. 2: Modulus (left panel) and phase (right panel) of the strange vector form factor obtained by solving a three-channel Muskhelishvili-Omnès equations system. Variation with the symmetry breaking parameter a(see Eq.(54)).

Definition of pole part of the scalar and vector form factors

We want to define the extrapolation of the scalar form factor to the 2nd Riemann sheet in t.
Scattering is elastic up to the $K\eta'$ threshold. The discontinuity across the cut is:

$$f_{0,1}^{K\pi}(t+i\epsilon) - f_{0,1}^{K\pi}(t-i\epsilon) = -2\sigma_{\pi K}(t+i\epsilon)T_{11}^{S,P}(t+i\epsilon)f_{0,1}^{K\pi}(t-i\epsilon)$$

$$\text{with } \sigma_{\pi K}(t) = 1/t\sqrt{((m_K+m_\pi)^2-t)(t-(m_K-m_\pi)^2)}$$

$$T_{11}^{S,P}(t+i\epsilon) - T_{11}^{S,P}(t-i\epsilon) = -2\sigma_{\pi K}(t+i\epsilon)T_{11}^{S,P}(t+i\epsilon)T_{11}^{S,P}(t-i\epsilon)$$

This allow us to find the extension of $f_{0,1}^{K\pi}$ on the 2nd Riemann sheet : $f_{0,1}^{\mathrm{II}}(t) = \dfrac{f_{0,1}^{K\pi}(t)}{1-2\sigma_{\pi K}(t)T_{11}^{S}(t)}$

which, by definition, must satisfy $f_0^{\mathrm{II}}(t-i\epsilon) = f_0^{K\pi}(t+i\epsilon)$ along the cut.

$$f_0^{\mathrm{pole}}(t) = \frac{f_0^{K\pi}(t_0)}{\alpha\,(t-t_0)} \qquad \alpha = dD(t)/dt|_{t=t_0}$$

Modulus of scalar form factor $f_0^{K\pi}$ compared with its pole part

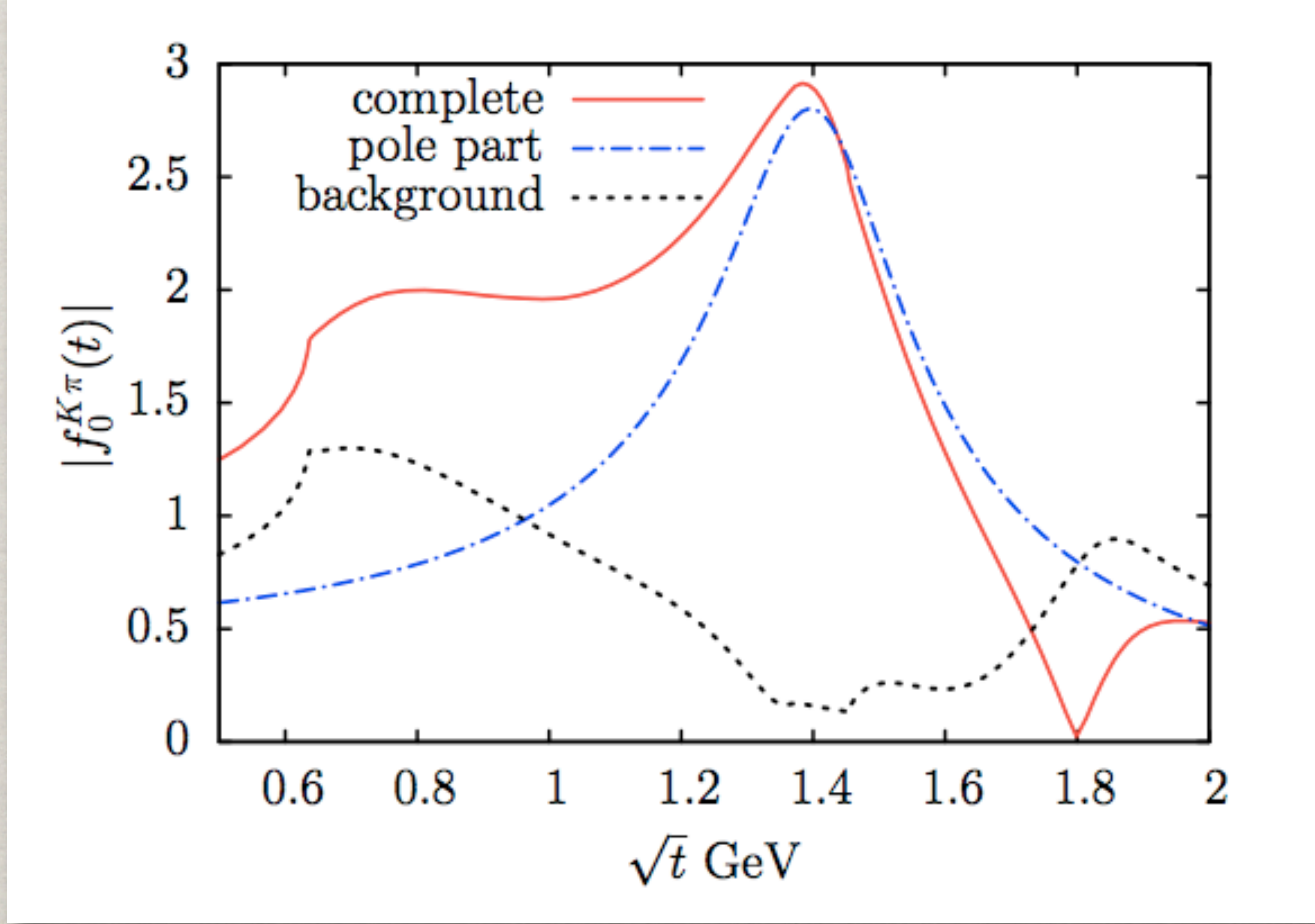

Modulus of the scalar form factor $f_1^{K\pi}$ compared with its pole part

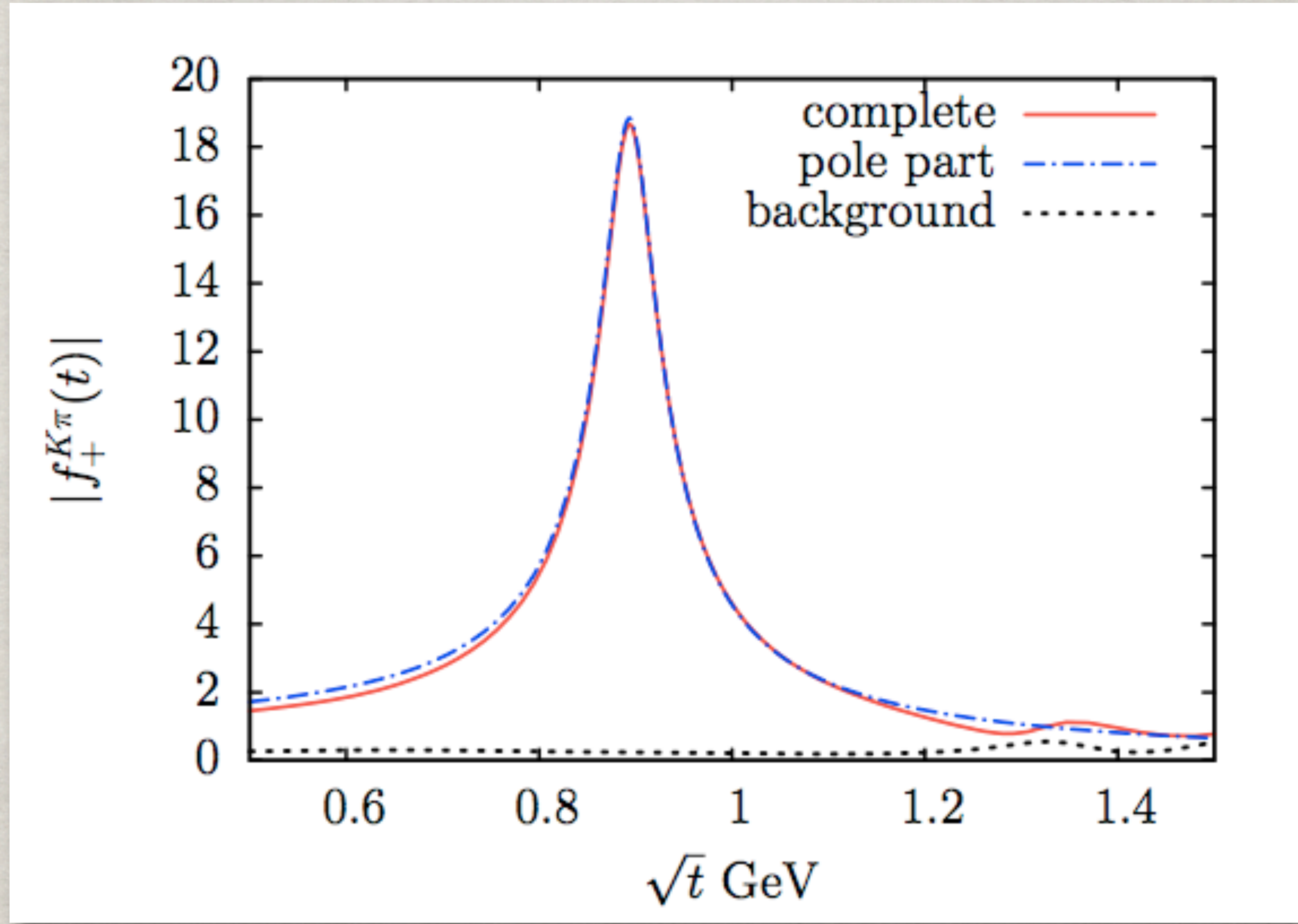

Results

Invariant $m_{\pi K}$ mass distributions

$$\frac{d^2\Gamma^-}{d\cos\theta\, dm_{K^-\pi^+}} = \frac{m_{K^-\pi^+}|\mathbf{p}_{\pi^+}|\ |\mathbf{p}_{\pi^-}|}{8(2\pi)^3 M_B^3}|\mathcal{M}^-|^2$$

$$\frac{d\mathcal{B}^-}{dm_{K^-\pi^+}} = \frac{1}{\Gamma_B^-}\frac{m_{K^-\pi^+}|\mathbf{p}_{\pi^+}|\ |\mathbf{p}_{\pi^-}|}{4(2\pi)^3 M_B^3}\left(|\mathcal{M}_S^-|^2 + \frac{1}{3}|\mathbf{p}_{\pi^+}|^2\ |\mathbf{p}_{\pi^-}|^2|\mathcal{M}_P^-|^2\right)$$

$$\frac{d\mathcal{B}^-}{d\cos\theta} = A + B\cos\theta + C\cos^2\theta$$

with the helicity angle related to $m_{\pi\pi}$:

$$\cos\theta = \frac{p_{\pi^+}\cdot p_{\pi^-}}{|p_{\pi^+}||p_{\pi^-}|}$$

Pion-kaon invariant mass distributions

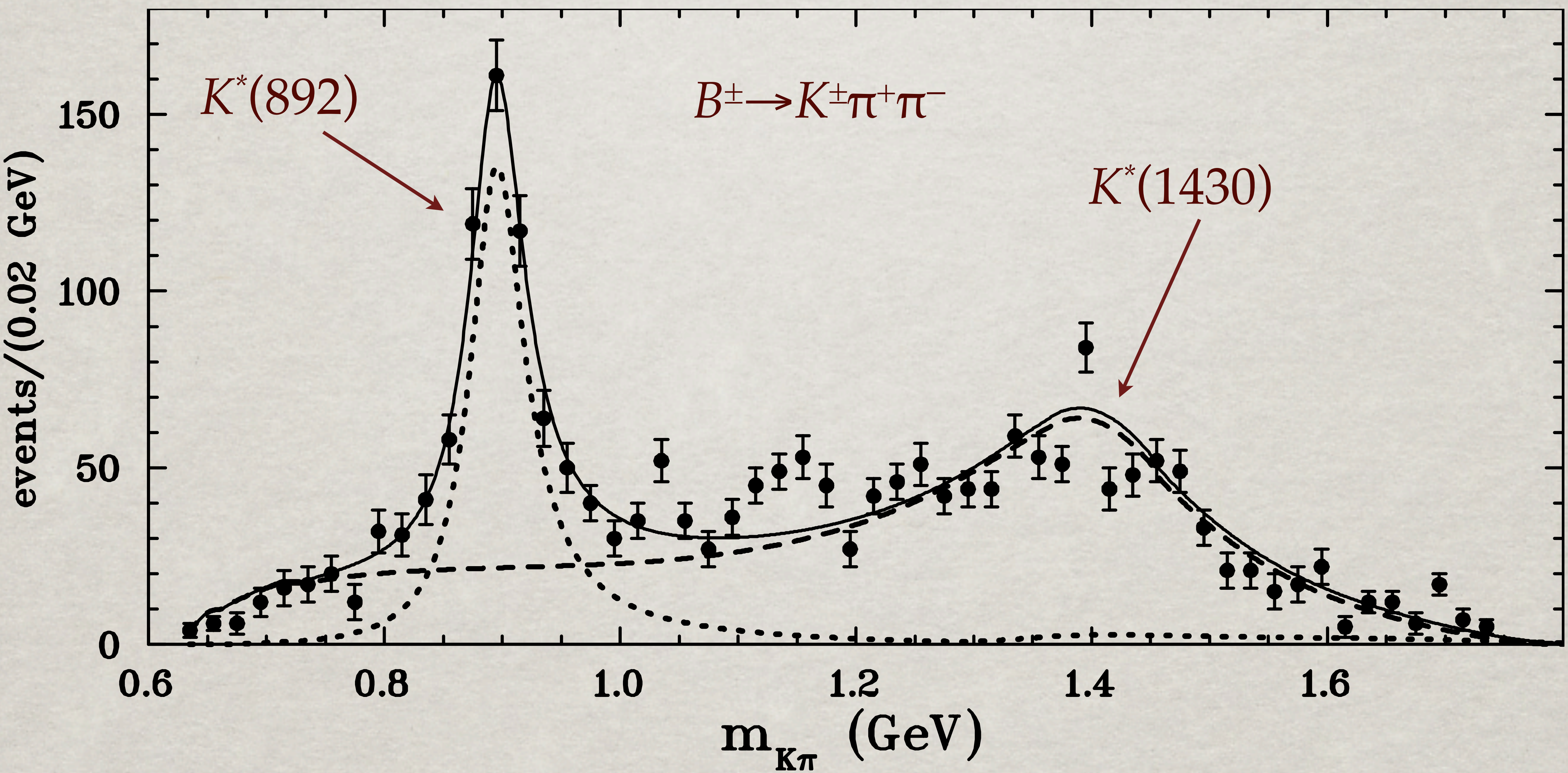

A. Garmash *et al*. (Belle), PRL 96, 251803 (2006)

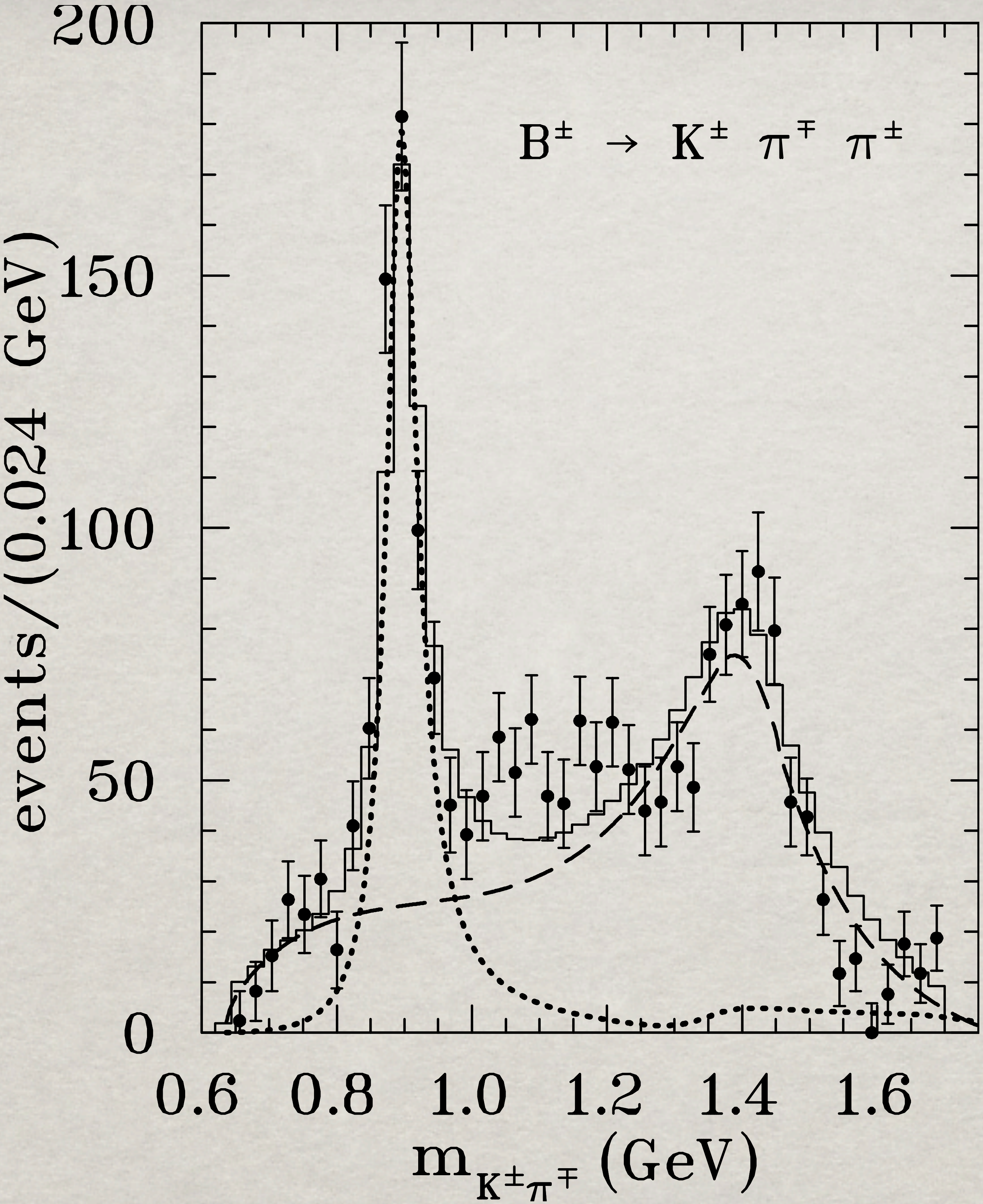

B. Aubert *et al*. (BaBar), Phys. Rev. D 78, 012004

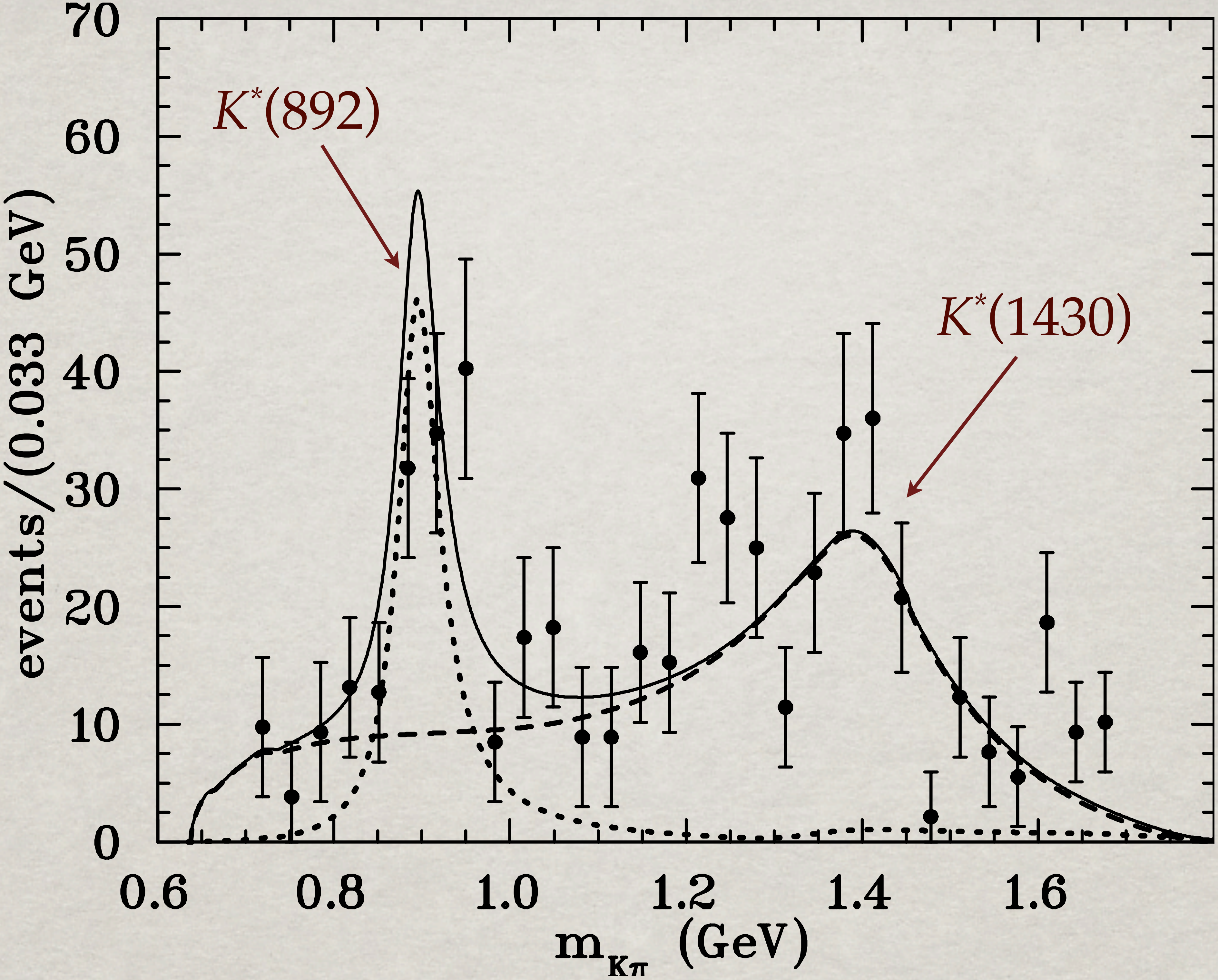

$B^0 \rightarrow K^0\pi^+\pi^-$, BaBar data, Phys. Rev. D 73, 031101(R) (2006)

$B^{\pm} \to K^{\pm}\pi^{+}\pi^{-}$ helicity distributions

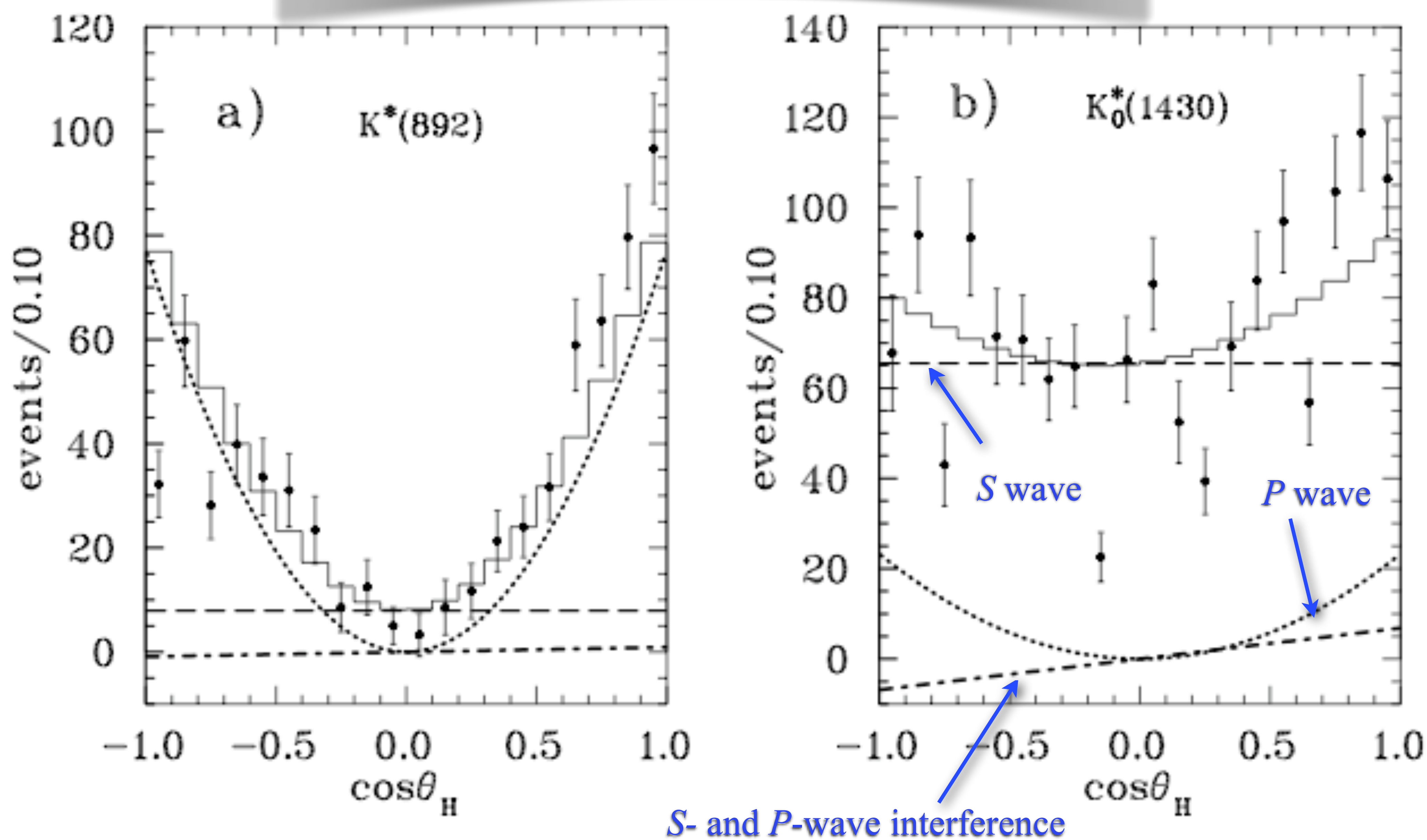

FIG. 7: Helicity angle distributions for $B^{\pm} \to K^{\pm}\pi^{\mp}\pi^{\pm}$ decays calculated from the averaged double differential distribution integrated over $m_{K^{\pm}\pi^{\mp}}$ mass from 0.82 to 0.97 GeV in the $K^*(892)$ case a) and from 1.0 to 1.76 GeV in the $K_0^*(1430)$ one b). Data points are from Ref. [5]. Dashed lines represent the S-wave contribution of our model, dotted lines that of the P-wave, the dot-dashed that of the interference term. The histograms corresponding to the sum of these three contributions.

For comparison helicity in $m_{\pi\pi}$ regions

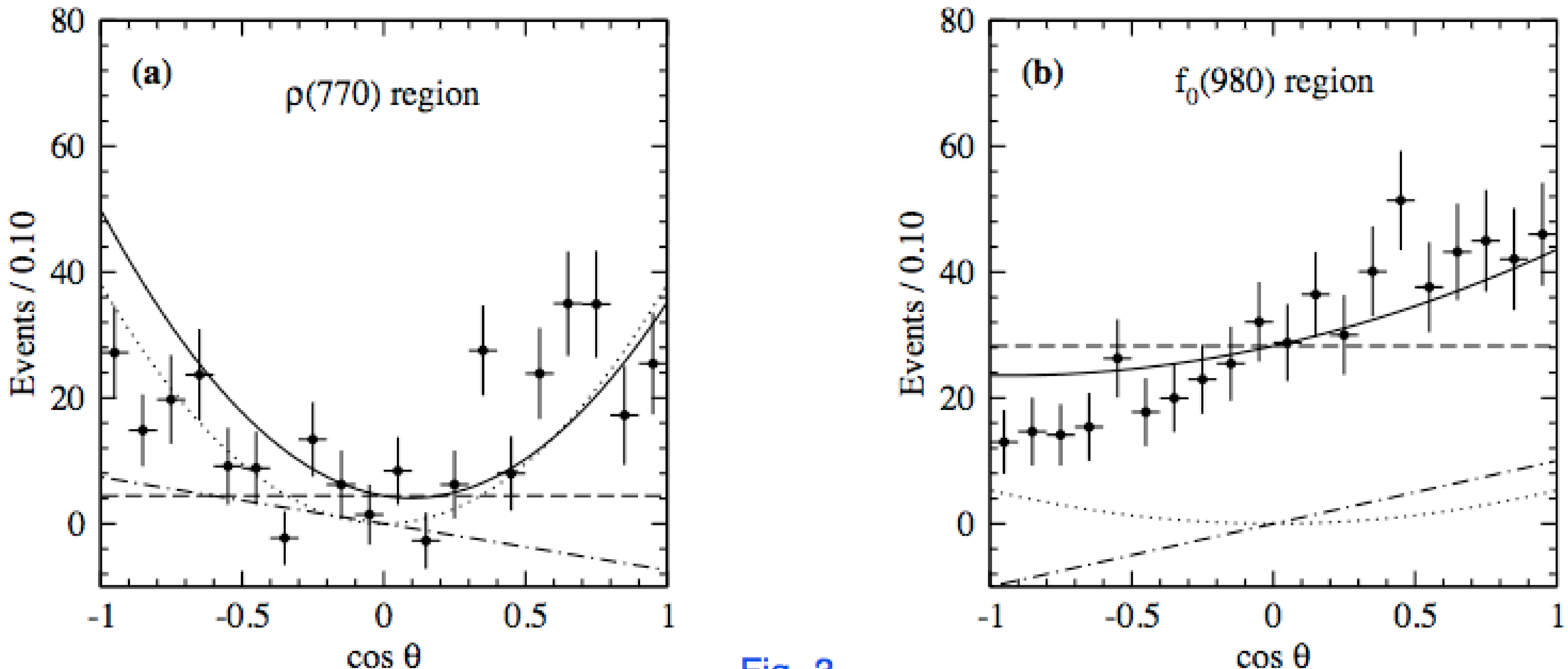

Fig. 3

(Integration 0.6 GeV < $m_{\pi\pi}$ < 0.9 GeV)

(Integration 0.9 GeV < $m_{\pi\pi}$ < 1.06 GeV)

– – – – S-wave ; · · · · · · P-wave ; —·—·— Interference ; ——— Total

Data from Belle [1]

B. El-Bennich *et al.*, Phys. Rev. D74, 114009 (2006)

Summary of branching ratio and *CP* asymmetry values for $m_{\pi K}$

TABLE III. Branching fractions for the $B \to K^*(892)\pi$ decays averaged over charge conjugate reactions in units of 10^{-6}. In the second column, giving the experimental branching ratios, the 2/3 factor arises from isospin symmetry. The values of the model calculated by the integration on $m_{K\pi}$ from 0.82 to 0.97 GeV are compared to the corresponding Belle and *BABAR* results given in the fourth column. Model errors stem from the phenomenological parameter uncertainties obtained through the minimization procedure. The last column corresponds to the model without phenomenological parameters.

Decay mode	$\mathcal{B}^{\rm exp}$	Ref.	$\mathcal{B}^{\rm exp}(0.82, 0.97)$	model	model $[c_i^p = 0]$
$B^- \to [\bar{K}^{*0}(892) \to K^-\pi^+]\pi^-$	6.45 ± 0.71	[6]	5.35 ± 0.59	5.73 ± 0.14	1.42
	7.20 ± 0.90	[11]	5.98 ± 0.75		
$\bar{B}^0 \to [\bar{K}^{*-}(892) \to \bar{K}^0\pi^-]\pi^+$	5.60 ± 0.93	[9]	4.65 ± 0.77	5.42 ± 0.16	1.09
	$\frac{2}{3}(11.7 \pm 1.30)$	[12]	6.47 ± 0.72		

TABLE IV. Direct *CP* asymmetries averaged over charge conjugate reactions. The values of the model, calculated over the $m_{K\pi}$ range from 0.82 to 0.97 GeV for the $K\pi$ *P*-wave and from 1.0 to 1.76 GeV for the *S*-wave, are compared to the Belle and *BABAR* results. Concerning the errors of the model and the last column, see the caption in Table III.

Decay mode	exp. (%)	Ref.	model (%)	model (%) $[c_i^p = 0]$
$B^- \to [\bar{K}^{*0}(892) \to K^-\pi^+]\pi^-$	-14.9 ± 6.8	[6]	-2.5 ± 1.3	1.4
	3.2 ± 5.4	[11]		
$B^- \to [\bar{K}_0^*(1430) \to K^-\pi^+]\pi^-$	7.6 ± 4.6	[6]		
$B^- \to (K^-\pi^+)_S\pi^-$	3.2 ± 4.6	[11]	5.4 ± 1.0	0.2
$\bar{B}^0 \to [\bar{K}^{*0}(892) \to \bar{K}^0\pi^-]\pi^+$	-14 ± 12	[12]	-19.6 ± 3.0	6.1
$\bar{B}^0 \to (\bar{K}^0\pi^-)_S\pi^+$	17 ± 26	[12]	-0.2 ± 1.3	-1.7

TABLE V. Branching fractions averaged over charge conjugate reactions $B \to (K\pi)_S\pi$ in units of 10^{-6}. The second column gives the experimental results. The predictions of our model, calculated by the integration of the $m_{K\pi}$ distribution over $m_{K\pi}$ from threshold (0.64 GeV) to 1.76 GeV, are compared to the corresponding Belle and *BABAR* results given in the fourth column. In the first two lines, the Belle branching fractions [6,9], calculated with a Breit-Wigner amplitude, are compared to our predictions obtained from the $K_0^*(1430)$ pole part of the scalar form factor (see Sec. IV B 2). In the last two lines we show the *BABAR* branching fractions [11,12] for $B \to (K\pi)_S\pi$ calculated, in their parametrization, with the part of the decay amplitude proportional to the $K\pi$ S-wave T-matrix. This is compared to the results of our model, where the $B \to (K\pi)_S\pi$ amplitude corresponds to the part proportional to the scalar form factor (see Sec. IV B 1). See caption of Table III for the factor of 2/3 in the first column, for the errors of the model and for the last column.

Decay mode	$\mathcal{B}^{\text{exp}}$	Ref.	$\mathcal{B}^{\text{exp}}(0.64, 1.76)$	model	model $[c_i^P = 0]$
$B^- \to [\bar{K}_0^{*0}(1430) \to K^-\pi^+]\pi^-$	32.0 ± 3.0	[6]	27.0 ± 2.5	11.6 ± 0.6	6.1
$\bar{B}^0 \to [\bar{K}_0^{*-}(1430) \to \bar{K}^0\pi^-]\pi^+$	30.8 ± 4.0	[9]	26.0 ± 3.4	11.1 ± 0.5	5.7
$B^- \to (K^-\pi^+)_S\pi^-$	24.5 ± 5.0	[11]	22.5 ± 4.6	16.5 ± 0.8	7.5
$\bar{B}^0 \to (\bar{K}^0\pi^-)_S\pi^+$	$\frac{2}{3}(28.2 \pm 7.5)$	[12]	17.3 ± 4.6	15.8 ± 0.7	7.1

Scalar form factor *vs.* BaBar parametrization

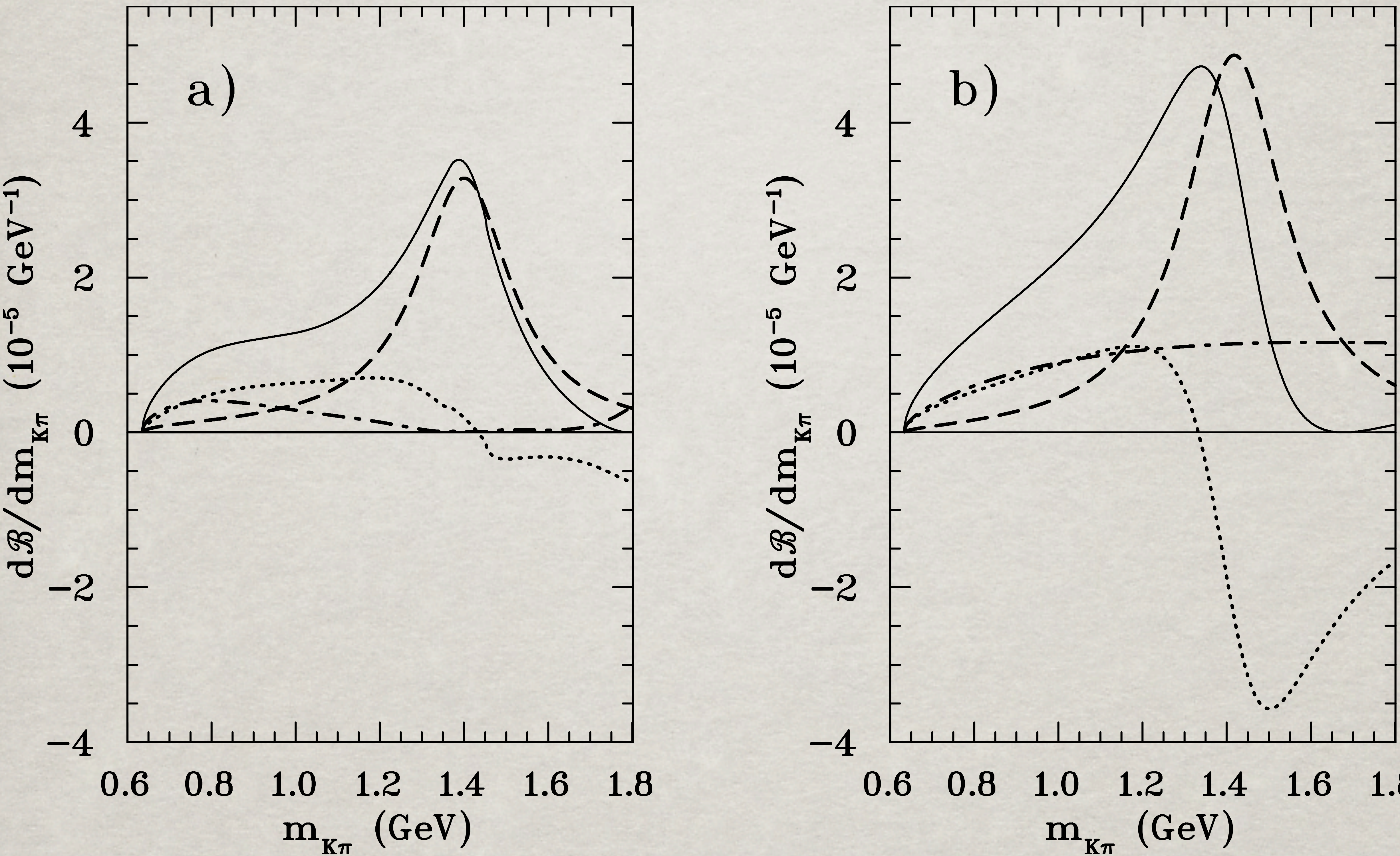

T-matrix.The dashed lines correspond to the resonant $K_0^*(1430)$ contributions, the dotted-dashed lines to the background, dotted lines to the interference and the solid lines to their sum.

Concluding remarks

- We have studied the contributions of pion-pion and pion-kaon scattering to the three-body $B \to K\pi\pi$ decay amplitude.

- These contributions explain partially the disagreement between the “two-body” QCD factorization approach (20% – 30% increase of branching ratios) and experimental branching ratios. They add strong phases that contribute to CP violation and are ***indispensable*** to explain interference effects seen in helicity distributions.

- At any rate, the quasi two-body approach allows for a calculation of the invariant mass distribution, which is more suitable with respect to the experimental analyses of Dalitz plots. We can provide a simple but rigorously unitary parametrization for $B \to (K\pi)_{S,P}\,\pi$ decays (diminishes ambiguities in experimental analyses).

THE END

Extra Material

Annihilation topologies

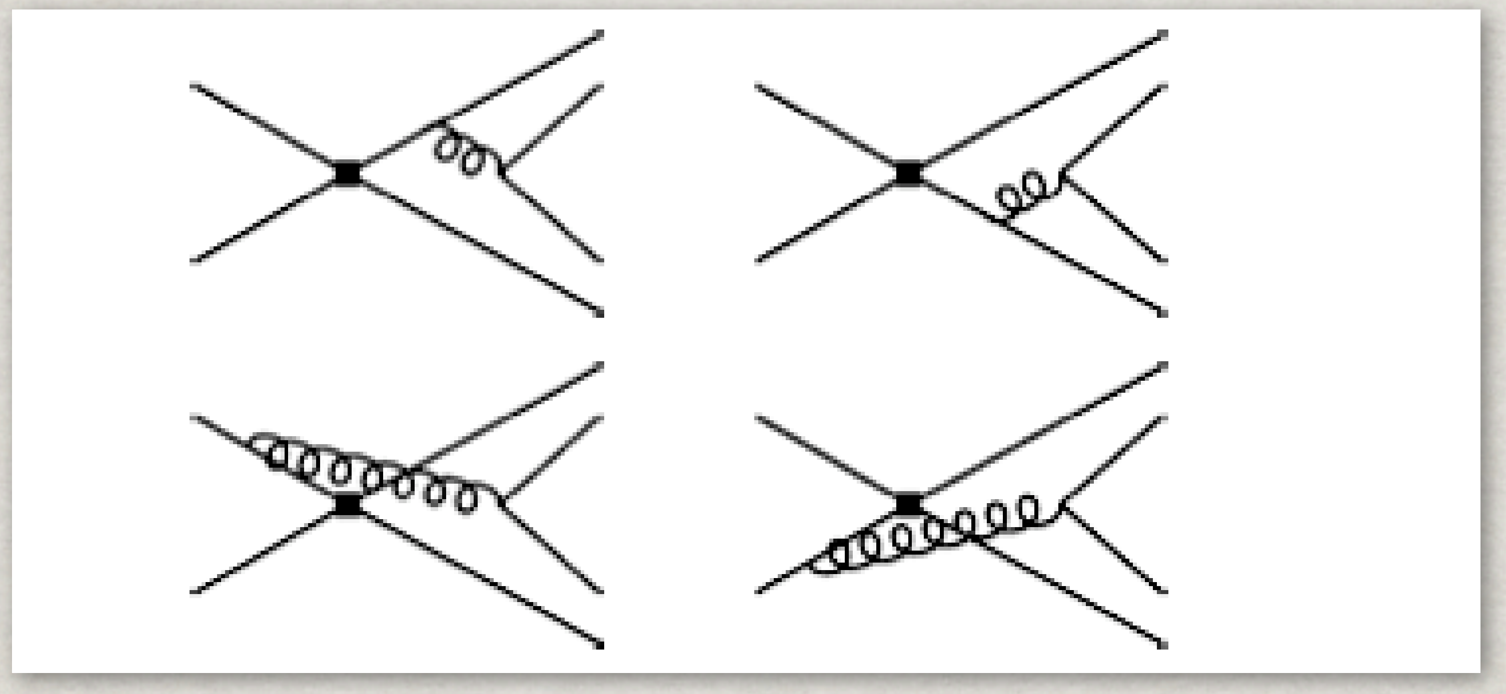

"What appears to you as annihilation may be a new beginning"
Arthur Schopenhauer, Die Welt als Wille und Vorstellung

These diagrams imply endpoint divergences due to the form of twist-3 light cone distribution:

$$\int_0^1 \frac{dx}{1-x}\,\phi_m(x) \to X_A \phi_m(1) \qquad \phi_m(x) \neq 0,\ x \to 1$$

$$X_A = 1 + \rho_A e^{i\varphi_A} \propto \ln\left(\frac{m_b}{\Lambda_{\rm QCD}}\right)$$ $\Rightarrow$ φ_A introduces a phenomenological strong phase $\rho_A < 1$.

Charming Penguins are interpreted as long-distance contributions

Penguin type diagram for the $B^- \to (K^-\pi^+)\pi^-$ decay

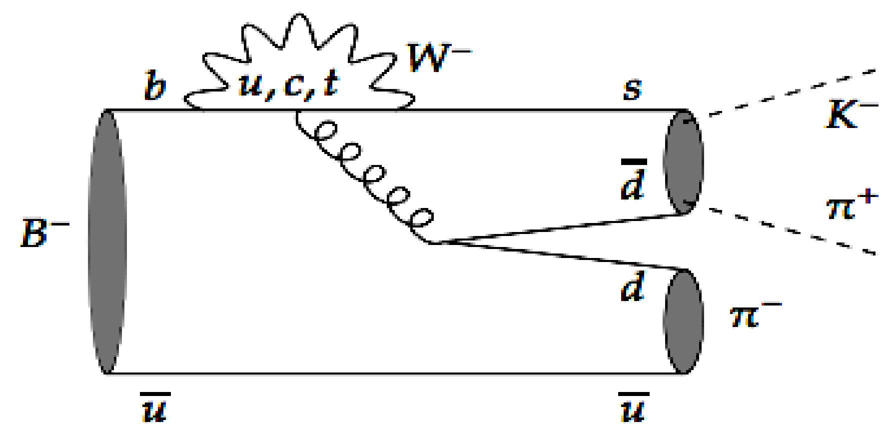

Long-distance amplitudes with c-quark in loop:

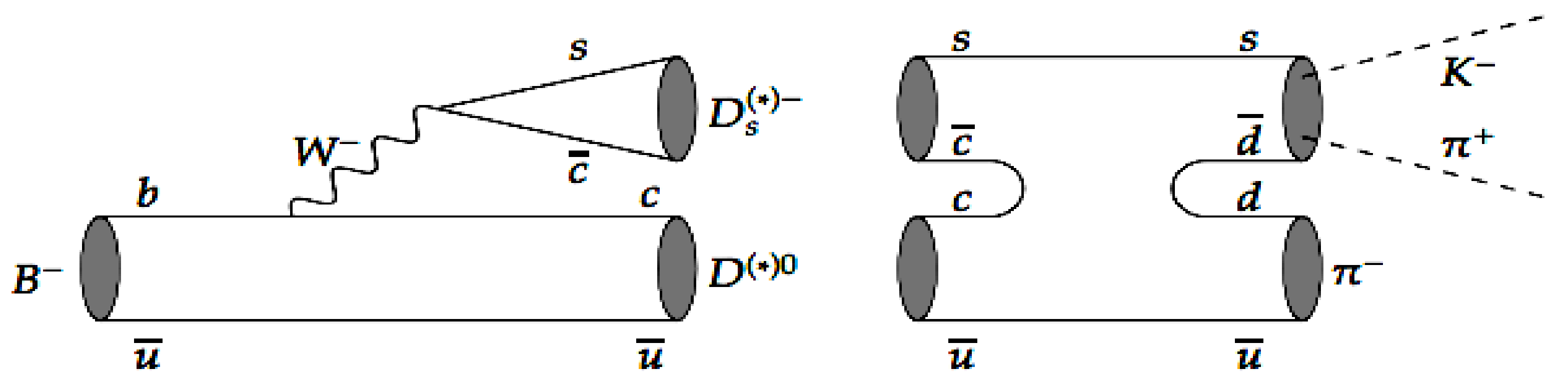

$$B^- \to D_s^- D^0 \xrightarrow[\left[c\bar{c}\ \text{annihilation}\right]]{} f_0(980)K^-$$

Strong phase of $B^{\pm} \to K^{\pm}\pi^{+}\pi^{-}$ decay amplitude

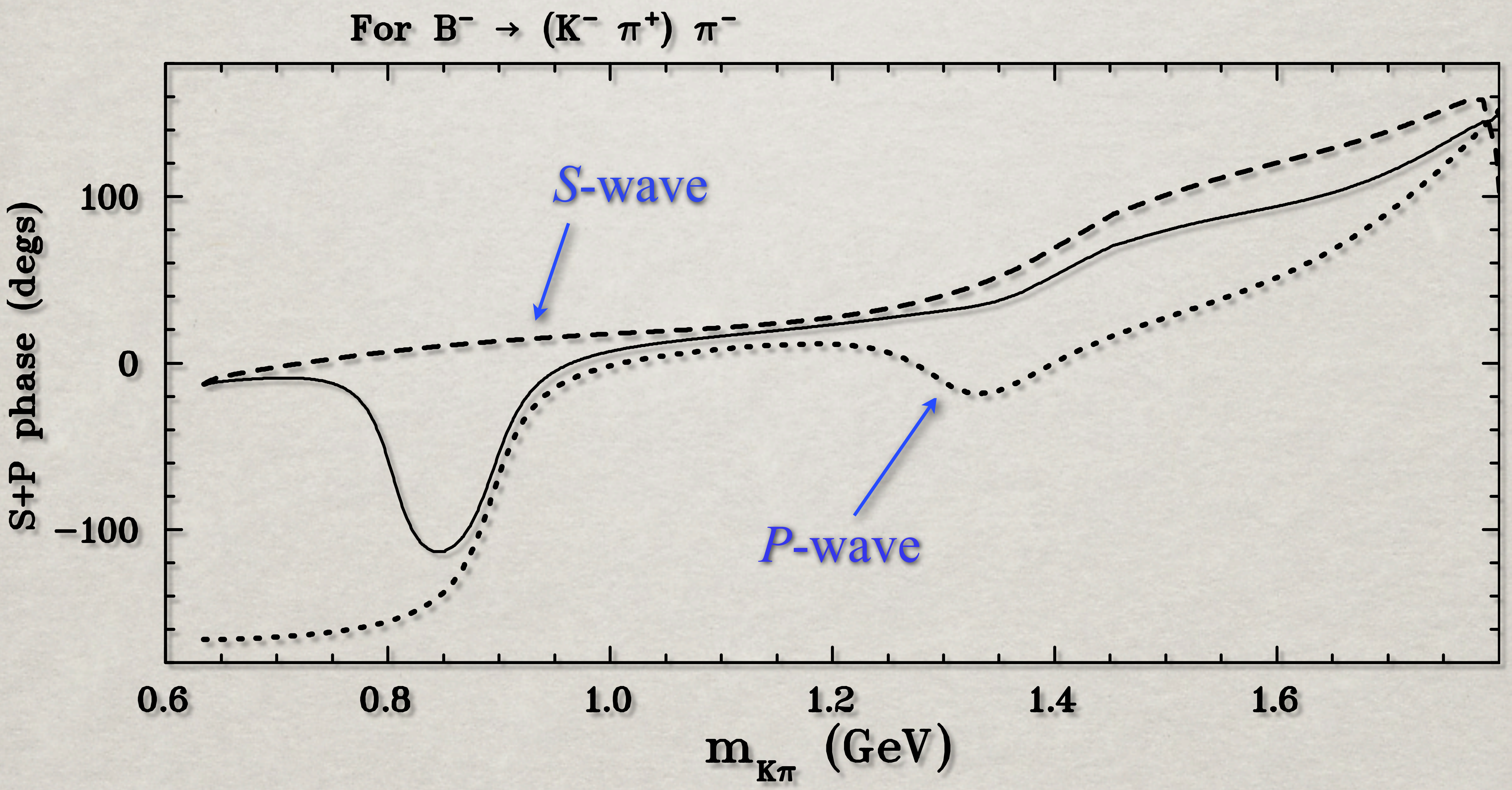

CP asymmetries

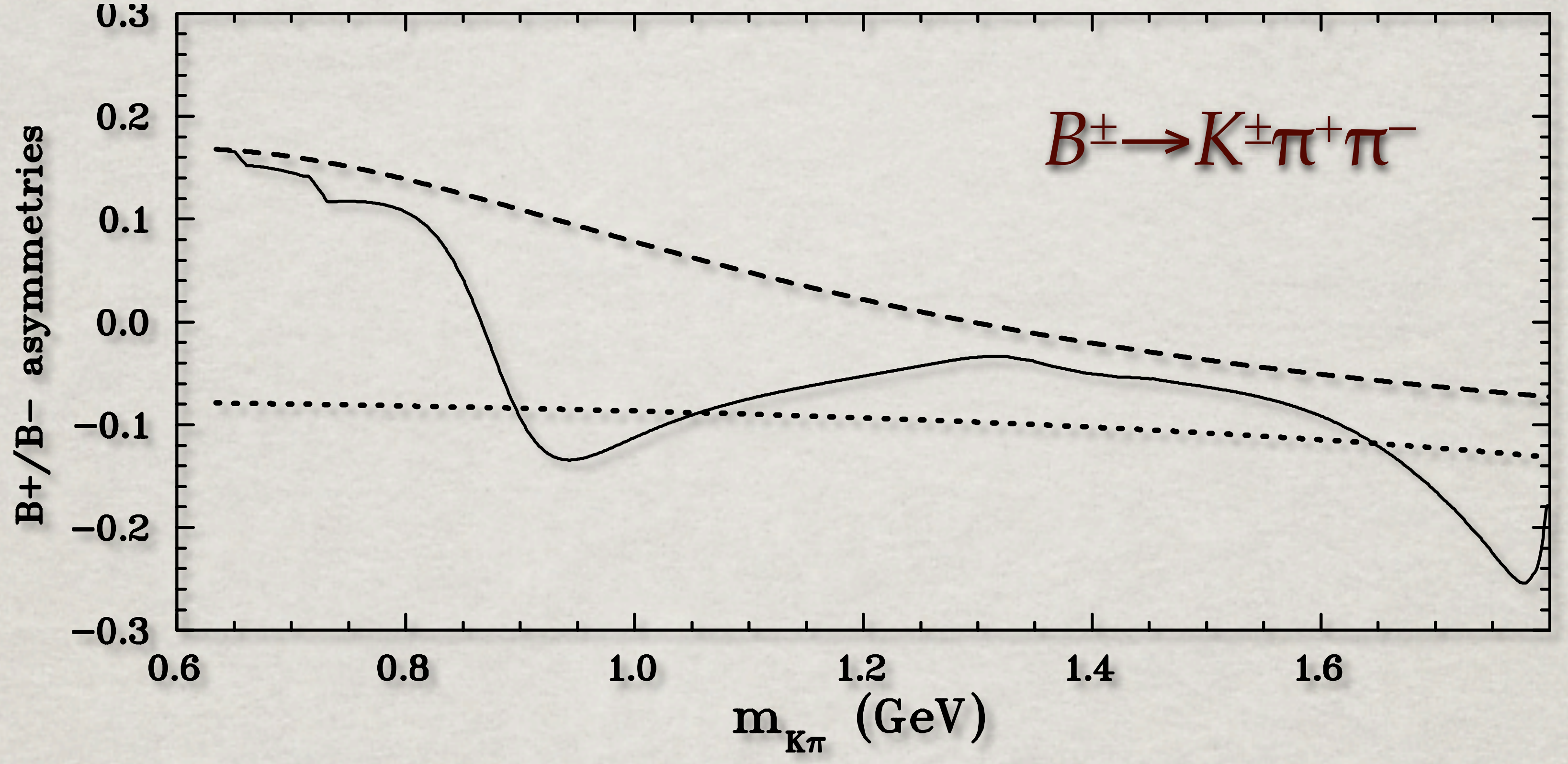

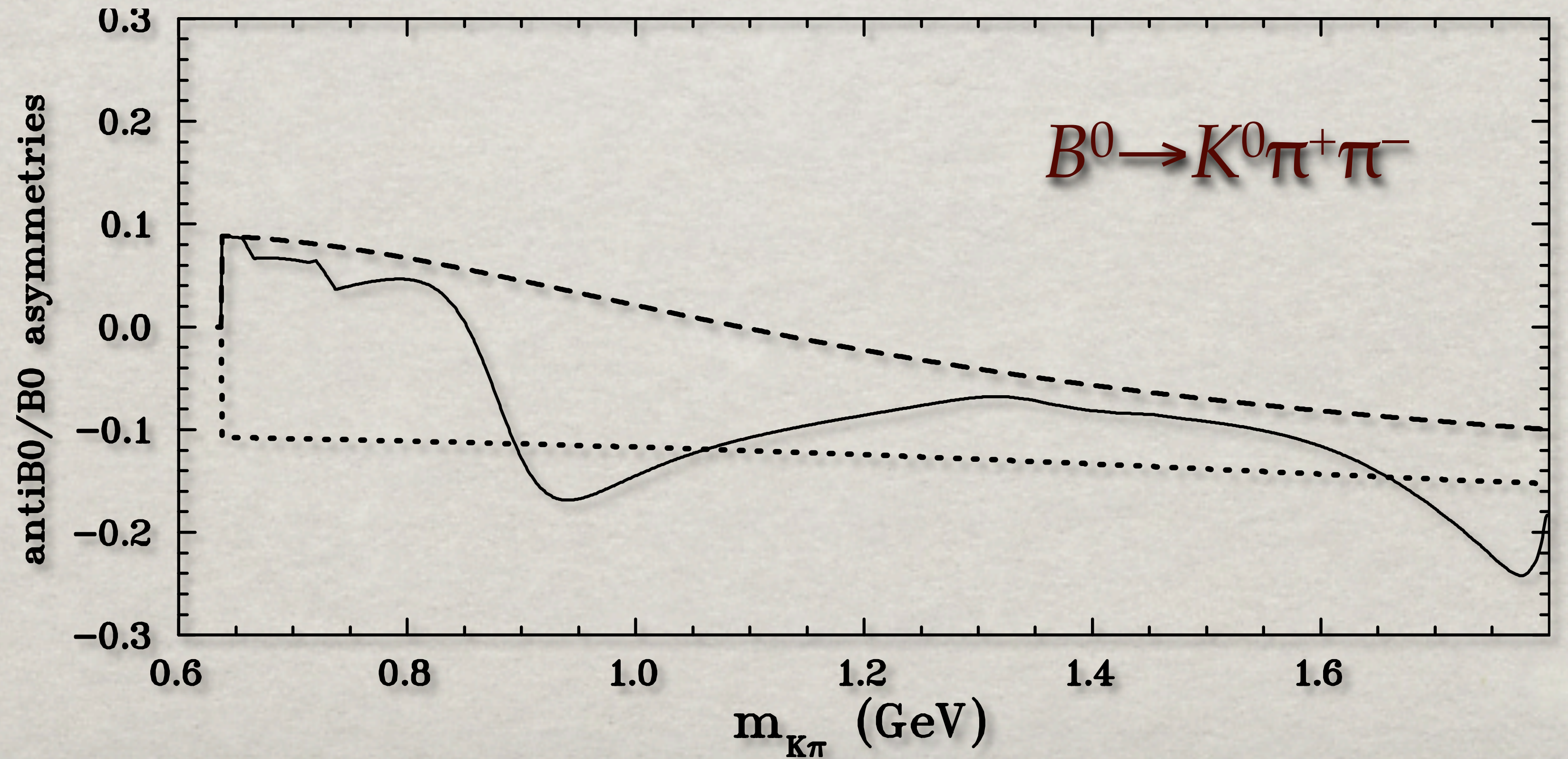

Quark-Line topologies for $B \to f_0(980)K$

Example:

$$\begin{cases} B^- \to (\pi\pi)_S K^- \\ B^- \to (KK)_S K^- \end{cases}$$

$$\left.\begin{array}{l} (\pi\pi)_S : \pi^+\pi^- \text{ or } \pi^0\pi^0 \\ (KK)_S : K^+K^- \text{ or } K^0\bar{K}^0 \end{array}\right\} \begin{array}{c} \text{Isospin zero} \\ \text{S-wave} \end{array}$$

For B^0 decays no tree diagram (a), only penguin diagrams similar to ones in (b) or (c)

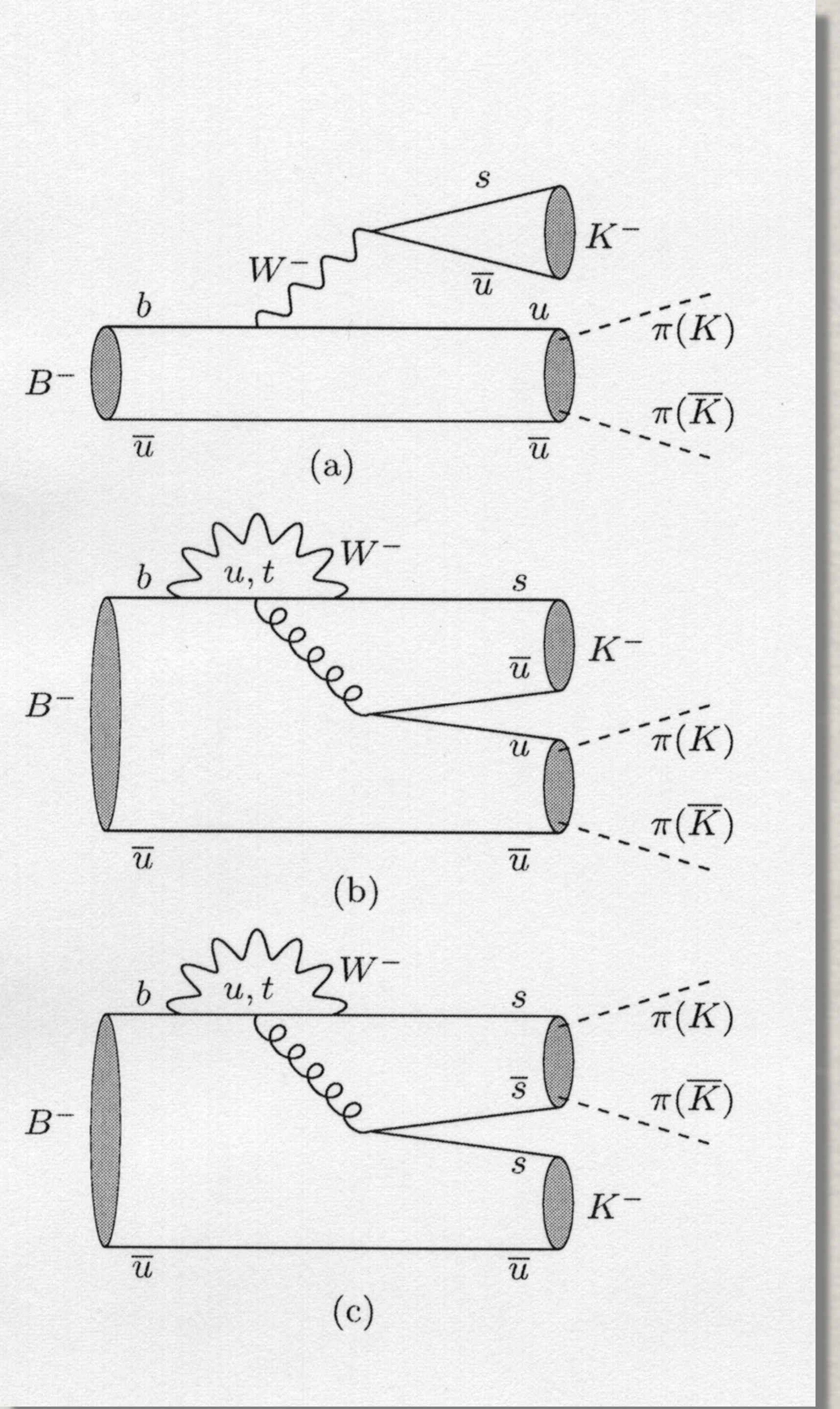

Form factors that contribute to "hadronic pollution"

$P \to S, P$ transition form factors (and similarly for $P \to V$) :

$$\langle M|\bar{q}\gamma^\mu(1-\gamma_5)b|B\rangle\rangle =$$
$$= \left[(p_B+p_M)^\mu - \frac{M_B^2-m_M^2}{q^2}q^\mu\right]F_1^{B\to M}(q^2) + \frac{M_B^2-m_M^2}{q^2}q^\mu F_0^{B\to M}(q^2),$$

The scalar and vector form factors have been estimated from lattice QCD, QCD sum rules, relativistic quark models and Dyson-Schwinger motivated approaches, see for example:

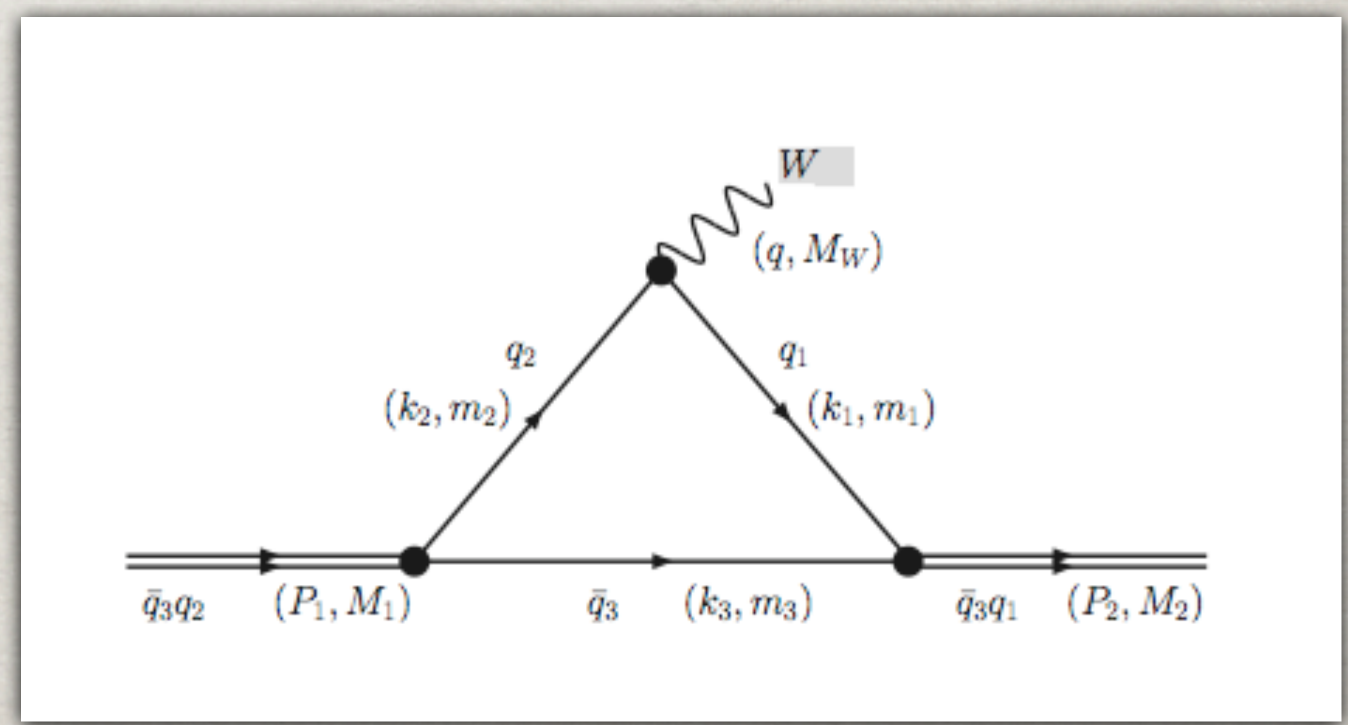

M. Ivanov, J. Körner, S. Kovalenko and C.D. Roberts, Phys. Rev. D76, 034018 (2007).

B. El-Bennich, O. Leitner, B. Loiseau and J.-P. Dedonder, Nucl. Phys. A790, 510 (2007).

P. Ball and R. Zwicky, Phys. Rev D71, 014015 (2005).